NASA TM-81911

NASA Technical Memorandum 81911

A SINGLE FRACTURE TOUGHNESS PARAMETER FOR
FIBROUS COMPOSITE LAMINATES

C. C. Poe, Jr.

March 1981

NASA

National Aeronautics and
Space Administration

Langley Research Center
Hampton, Virginia 23665
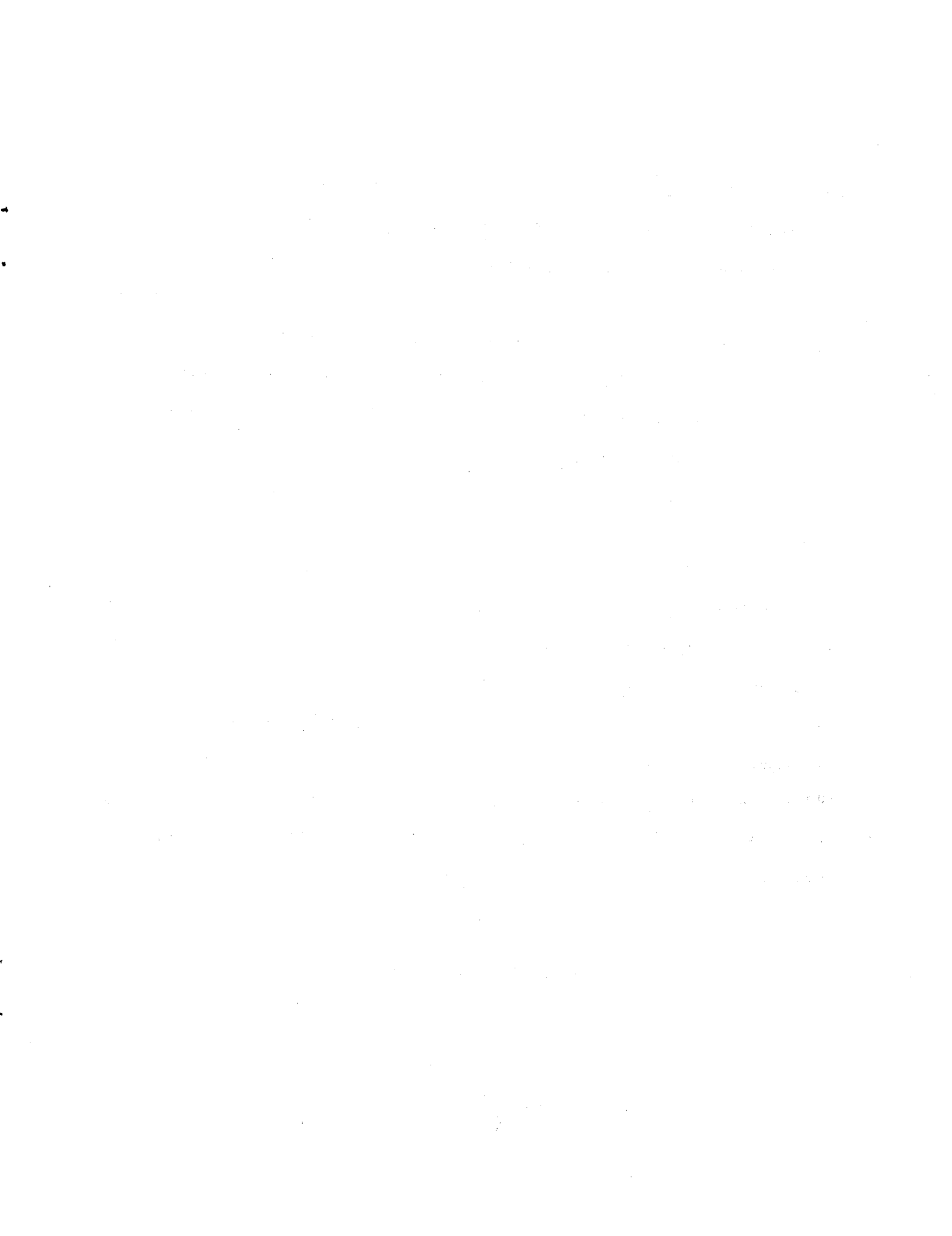
A SINGLE FRACTURE TOUGHNESS PARAMETER FOR

FIBROUS COMPOSITE LAMINATES

C. C. Poe, Jr.
NASA Langley Research Center
Hampton, Virginia 23665

ABSTRACT

A general fracture toughness parameter Q_c was previously derived and verified to be a material constant, independent of layup, for centrally cracked boron/aluminum composite specimens. The specimens were made with various proportions of $0°$ and $±45°$ plies. Moreover, a limited amount of data indicated that the ratio Q_c/ε_{tuf}, where ε_{tuf} is the ultimate tensile strain of the fibers, might be a constant for all composite laminates, regardless of material and layup. In that case, a single value of Q_c/ε_{tuf} could be used to predict the fracture toughness of all fibrous composite laminates from only the elastic constants and ε_{tuf}.

To verify that Q_c/ε_{tuf} is indeed a constant, values of Q_c/ε_{tuf} were calculated for centrally cracked specimens made from graphite/polyimide, graphite/epoxy, E-glass/epoxy, boron/epoxy, and S-glass-graphite/epoxy materials with numerous $\left[0_i/±45_j/90_k\right]$ layups. The data are presented herein. Within ordinary scatter, the data indicate that Q_c/ε_{tuf} is a constant for all laminates that did not split extensively at the crack tips or have other deviate failure modes.

Using a single value of Q_c/ε_{tuf} for all the layups and materials, strengths were predicted for the test specimens. The predicted and test values agree well except for laminates that split extensively. Then, the predicted strengths are usually conservative.

INTRODUCTION

Fibrous composite materials like graphite/epoxy are light, stiff, and strong. They have great potential for reducing weight in aircraft structures. However, fibrous composite laminates are usually notch sensitive and lose much of their original strength when damaged. Low-velocity impact damage caused by dropped tools, runway debris, birds, et cetera, is of particular concern. Thus, designers need to know the fracture toughness of composite laminates in order to design damage tolerant structures. Because composite laminates can be made with many different materials and layups, testing to determine the fracture toughness of each combination would be prohibitively expensive. Thus, a single fracture toughness parameter that can be used to predict the fracture toughness of all laminates, at least those of interest to the designer, is greatly needed.

In reference 1, a general fracture toughness parameter Q_c was derived and verified to be a material constant, independent of layup, for centrally cracked boron/aluminum (B/Al) sheet specimens. The sheets had various proportions of 0° and ±45° plies. The fracture toughness of each layup was expressed as the critical stress-intensity factor K_Q. The material constant Q_c, which defines the critical level of strains in the principal load-carrying plies, is proportional to K_Q. The equation for the constant of proportionality depends only on the elastic constants of the laminate and the orientation of the principal load-carrying fibers.

Since the elastic constants can be predicted quite well, so then can the constant of proportionality. Consequently, Q_c can be determined from tests of one layup, and K_Q can then be predicted for other layups of the same material.

2

Also in reference 1, the ratios of Q_c to ε_{tuf}, where ε_{tuf} is the ultimate tensile strain of the fibers, were shown to be equal for the $\left[0_i/\pm45_j\right]$ B/Al layups and for $[0/\pm45/90]$ layups made from graphite/epoxy (Gr/Ep), boron/epoxy (B/Ep), and E-glass/epoxy (E-Gl/Ep). If this is indeed true for all layups and materials, the fracture toughness of all fibrous composite laminates can be predicted from only tensile properties of unidirectional laminates.

The "point stress" criterion of Whitney and Nuismer (ref. 2) is also suggested by some to be a single fracture toughness parameter for composite materials. However, most people limit the "point stress" criterion to fiber-dominated layups. (In ref. 1, the general fracture toughness parameter predicted the fracture toughness of [±45] B/Al laminates quite well in spite of the non-linear stress-strain behavior.) Even for fiber-dominated layups, the "point stress" criterion and the general fracture toughness parameter can give quite different results, depending on the layup.

To verify that Q_c/ε_{tuf} is a constant for fibrous composite materials, values of Q_c/ε_{tuf} are presented herein for a large amount of test data. The specimens contained central crack-like slits. The test data, which included the B/Al data in reference 1, represent 44 combinations of 6 different materials and numerous $\left[0_i/\pm45_j/90_k\right]$ layups. Hybrid and matrix-dominated layups are included. Within ordinary scatter, the test data verify that Q_c/ε_{tuf} is a constant for all of the laminates that did not split extensively at the crack tips or have other deviate failure modes. Splitting elevated the values of Q_c. Then, to show that strengths can be predicted with a single value of Q_c/ε_{tuf} using only tensile properties, measured and predicted strengths are compared for many of the specimens. They usually agreed except when laminates split. Then, the predictions were usually conservative.

LIST OF SYMBOLS

a	half-length of crack-like slit, m
a_o	characteristic distance for "average stress" criterion, m
COD	crack-opening displacement measured midway between the ends of the slit, m
d_o	characteristic distance for "point stress" criterion, m
$\bar{d}_o$	characteristic distance for general fracture toughness parameter, m
E	Young's modulus, Pa
F_{tu}	ultimate tensile strength of laminate (uncracked specimen), Pa
G	shear modulus, Pa
K_Q	critical stress-intensity factor (fracture toughness), $Pa\sqrt{m}$
K_{Qe}	elastic critical stress-intensity factor, $Pa\sqrt{m}$
N	total number of values
n_i	i^{th} value
Q_c	general fracture toughness parameter, $\sqrt{m}$
S	gross laminate stress, Pa
S_c	stress at failure (strength) of cracked specimens, Pa
W	width of specimen, m
ε_c	far-field (remote) axial strain at failure
ε_{tu}	ultimate tensile strain of laminate (uncracked specimen)
ε_{tuf}	ultimate tensile strain of fibers
ε_1	strain in the fiber direction
ν	Poisson's ratio
ξ	functional that depends on orientation of principal load-carrying plies
ρ	size of crack-tip damage, m

4

Subscripts:

c   failure

net   based on net area rather than gross area

x,y   Cartesian coordinates (The x-direction is parallel to the slit and

          transverse to the 0° fibers.)

FAILURE MODES IN COMPOSITE LAMINATES

Test results for centrally cracked sheet specimens made of boron/aluminum

(B/Al) were reported in reference 1. The sheets were made with various propor-

tions of 0° and ±45° plies, including both [0] and [±45] layups. (The 0° plies

are aligned with the loading direction, which is transverse to the crack-like

slit.) On the macroscopic scale, the specimens failed largely by self-similar

crack extension, even the [±45] specimens.

Radiographs of the specimens indicated that only 0° fibers, or ±45° fibers

in [±45] laminates, began breaking at the ends of crack-like slits before over-

all failure. The breaking began at loads corresponding to about 80 percent of

the eventual strength. The breaks progressed from fiber to fiber, in effect

extending the slit in those plies. After the breaks had progressed ahead of

the slit ends a distance of about 1.5 mm, the specimen failed catastrophically.

Except for [±45] laminates, the 0° plies are the principal load-carrying plies,

that is, they carry more of the total load than the ±45° plies could carry

alone. In [±45] laminates, of course, the ±45° plies are the principal load-

carrying plies. Therefore, the overall failures were precipitated by unstable

extension of the crack-like slit in the principal load-carrying plies.

Tests also indicate that Gr/Ep laminates fail the same way. A

$[45/0/-45/90]_S$ Gr/Ep specimen was loaded to 95 percent of its estimated

5

strength, X-rayed, unloaded, and destructively examined. The photographs to the right in figure 1 show the second and third plies (viewed normally) near the slit end. Each ply was photographed after successively sanding away the outer ply. Broken fibers and small splits (matrix cracks) are clearly visible in the 0° ply. The 0° fibers are broken ahead of the slit end for a distance of approximately 3 mm. Notice that the damage in the -45° ply, which consists mainly of splits, coincides with the damage in the 0° ply.

A radiograph of the same area is also shown in figure 1. The dye TBE was used to enhance the image of the damage. The dark region indicates delaminations. The dark ±45° lines emanating from the slit end indicate splits in the ±45° plies. Faint lines to the right of and parallel to the slit indicate splits in the 90° plies. Because the breaks in the 0° fibers coincide with the damage in the -45° plies, the 0° fiber breaks were not revealed by the radiograph.

Figure 2 shows how crack-opening displacements (COD) also indicate that the failure of principal load-carrying fibers precipitates the overall failure of Gr/Ep laminates. The specimen is similar to that in figure 1, but twice as thick. For a very wide isotropic specimen, the COD midway between the slit ends is given by

$$COD = 4aS/E \tag{1}$$

Because the 0° plies contribute the most to the axial stiffness of the laminate, 0° fiber breaks at the slit ends will affect the COD much as an increase in slit length. Replacing a by $a + \rho$ in equation (1), where ρ is the extent of 0° fiber breaks, and solving for ρ,

$$\rho = 2a\left[(COD/S)/(COD/S)_o - 1\right] \tag{2}$$

6

where $(COD/S)_o$ is the initial compliance and (COD/S) is the compliance after 0° fibers break.

The values of ρ, calculated with equation (2), along with the COD measurements are plotted against applied stress in figure 2. For convenience, the applied stress was divided by the strength. The initial compliance in equation (2) was not measured from the COD curve because the initial part was somewhat erratic. Instead, it was calculated with equation (1). The COD jumped three times during the test. A discrete "pop" was audible each time. The smoothness of the COD curve and the absence of audible noise indicate that the crack-tip damage probably did not extend between jumps. Thus, in figure 2, the damage size ρ is shown as a constant between COD jumps. The calculated value of ρ after the last COD jump is 1.9 mm.

Radiographs made before the first COD jump (corresponding to a load of 43 percent of the strength) and immediately after each jump are also shown in figure 2. The TBE dye was used to enhance the image of the damage. The radiographs taken at the two largest loads reveal an apparent extension of the slit that could be 0° fiber breaks. The length of the extension is about equal to the ρ calculated from the COD curve. Thus, damage in the contiguous plies here may not coincide as it did in figure 1.

The results in figure 2 indicate that COD measurements may be a relatively simple and inexpensive method, at least compared to radiography, for monitoring crack-tip damage during a fracture test. As shown subsequently, fracture tests cannot be properly interpreted without knowing the type and size of crack-tip damage.

In contrast to the quasi-isotropic laminates shown in figures 1 and 2, laminates with a larger proportion of 0° plies, or with groups of 0° plies, can

7

develop very long splits at the slit ends in 0° plies. In some laminates, the splits extend clear to the specimen ends (grips) well before complete failure. Shear-lag analyses (e.g., refs. 3 and 4) indicate that splits can significantly reduce local fiber stresses and, consequently, can ameliorate the loss of strength due to a crack-like slit. (Of course, when splits extend to the specimen ends, the stress concentration factor is, for all intents and purposes, reduced to unity for very wide specimens.) The matrix shear stresses at the split ends are reduced by non-0° plies, which bridge the splits. The shear stresses are further reduced by dispersing the 0° plies among the non-0° plies rather than grouping them together. Therefore, the size of the splits in the 0° plies depends on the proportion of non-0° plies and their arrangement.

Although epoxy laminates can split, B/Al laminates usually do not (ref. 1). The aluminum matrix is much stronger and more ductile than the epoxy matrix. Even so, the 0° B/Al specimens do develop long yield zones due to the large matrix shear stresses. (The shear-lag analyses indicate that matrix yielding also reduces local fiber stresses, but not as much as splits.)

Epoxy laminates with S-glass fibers which have ultra-large ultimate tensile strains (0.028) also tend to split. The radiographs in figure 3 indicate that a $\left[45_{Gr}/0_{Gl}/-45_{Gr}/0_{Gl}\right]_{2S}$ S-glass-graphite/epoxy (S-Gl-Gr/Ep) hybrid specimen developed long splits before overall failure, whereas an all-Gr/Ep specimen did not appear to split at all. Based on the net-section area, the strength of the cracked hybrid specimen is nearly equal to that of an uncracked specimen. Thus, the splits probably extended to the specimen ends (grips). The hybrid specimen did not begin splitting until the stress reached about 123 percent (294 MPa) of the strength of the all-Gr/Ep specimen. Therefore, the hybrid specimen would not have split had its strength not been so much larger (about 150 percent) than

8

that of the all-Gr/Ep specimen. (Of course, the large strength of the hybrid specimen was partly due to the split itself, as noted previously.)

DERIVATION OF THE GENERAL FRACTURE TOUGHNESS PARAMETER Q_c

The test results in the previous section indicate that the failure of composite laminates is precipitated by failure of the principal load-carrying fibers just ahead of the crack tips. Therefore, overall failure should occur when the strains in the principal load-carrying fibers reach a critical level. These strains were derived in reference 1 for an axially loaded, specially orthotropic sheet containing a central crack-like slit. The strains were expressed in terms of the stress-intensity factor using laminate analysis. This analysis is valid when crack-tip damage is small compared to crack length. The critical level of fiber strains was then defined by a general fracture toughness parameter Q_c, which is proportional to the critical value of the stress-intensity factor K_Q. The constant of proportionality depends only on the elastic constants and the orientation of the principal load-carrying fibers. Since the critical level of fiber strains should depend only on the strain capability of the fibers, Q_c should be a fiber property, independent of layup. The test data in reference 1 for the various B/Al layups verified the critical strain level and, hence, Q_c is reasonably independent of the proportion of 0° and ±45° plies.

The equation for Q_c (ref. 1) is

$$Q_c = K_Q \xi / E_y \qquad (3)$$

where ξ is a functional that depends on the orientation of the principal load-carrying fibers and E_y is Young's modulus in the 0°-fiber direction (also the loading direction). When 0° fibers are the principal load-carrying fibers,

9

$$\xi = 1 - \nu_{yx} \sqrt{E_x/E_y} \tag{4}$$

and when ±45° fibers are the principal load-carrying fibers,

$$\xi = \frac{1}{2}\left(1 - \nu_{yx} \sqrt{E_x/E_y}\right)\left(1 + \sqrt{E_y/E_x}\right) \tag{5}$$

The E_x and ν_{yx} are the Young's modulus transverse to the 0°-fiber direction and the major Poisson's ratio, respectively. The major Poisson's ratio ν_{yx} gives the ratio of transverse-to-longitudinal strain when a uniaxial load is applied in the 0°-fiber direction. (Values of ξ can be calculated for other principal fiber orientations using the equation in ref. 1.)

Because Q_c is a fiber property that depends on the strain capability of the fibers in the principal load-carrying plies, Q_c should also be proportional to the ultimate tensile strain of the fibers ε_{tuf}. Indeed, a preliminary study in reference 1 indicated that Q_c/ε_{tuf} is approximately equal for the various B/Al layups and for quasi-isotropic epoxy layups made from graphite, boron, and E-glass fibers.

It is important to note that Q_c/ε_{tuf} squared is proportional to a "characteristic distance," like that in the "point stress" criterion of Whitney and Nuismer (ref. 2). However, the "point stress" criterion is limited to fiber-dominated layups, but the general fracture toughness parameter (ref. 1) is not. Moreover, even for fiber-dominated layups, the appendix shows that the "point stress" criterion and general fracture toughness parameter can give quite different results, depending on the layup.

A REPRESENTATIVE VALUE OF Q_c/ε_{tuf}

Method for Calculating Q_c/ε_{tuf}

Values of Q_c and Q_c/ε_{tuf} were calculated for six different composite materials and numerous layups. The results are given in table I, along with the ultimate tensile strength of each material and layup. All of the layups are symmetric and balanced, and belong to the $\left[0_i/\pm45_j/90_k\right]$ family. The different materials are graphite/epoxy (Gr/Ep), graphite/polyimide (Gr/Pi), E-glass/epoxy (E-Gl/Ep), boron/epoxy (B/Ep), S-glass-graphite/epoxy (S-Gl-Gr/Ep), and boron/aluminum (B/Al). The Gr/Ep laminates were made from T300/5208, T300/934, and T300/SP-286 material systems.

The values of Q_c and Q_c/ε_{tuf} in table I are averages for all specimens made of a given material and layup. The test data used to calculate Q_c were taken from references 1, 5 through 11, and table II. Table II contains results of individual tests conducted by the author for several Gr/Ep layups. The specimens were axially loaded and contained central, crack-like slits. The data generally include duplicated tests of specimens with several crack lengths and sometimes with several widths. In all, average values of Q_c/ε_{tuf} are reported for 44 combinations of material and laminate orientation.

Except for B/Al laminates, the values of Q_c in table I were calculated with equations (3) through (5). For B/Al, the values of Q_c were taken directly from reference 1, where they were calculated with failing strains in order to eliminate nonlinear stress-strain effects.

For axially loaded specimens with central crack-like slits, the K_Q values in equation (3) were calculated assuming

$$K_Q = S_c\sqrt{\pi(a + \rho_c)\ \sec\ (\pi a/W)} \tag{6}$$

where S_c is the strength, a is the half-length of the crack-like slit, W

is the specimen width, ρ_c is the size of damage at the slit ends at failure,

and $\sqrt{\sec (\pi a/W)}$ is a widely used isotropic finite-width correction factor.

The isotropic finite-width correction factor was used for convenience since

finite-element calculations indicated that the effect of anisotropy for the lay-

ups in tables I and II was small, usually less than 5 percent. The ρ_c in

equation (6) was determined so that equation (6) predicts the ultimate tensile

strength when there is no crack--just like in reference 1. Substituting

$S_c = F_{tu}$ and $2a = 0$ into equation (6) and solving for ρ_c,

$$\rho_c = \left(K_Q/F_{tu}\right)^2 \Big/ \pi \qquad (7)$$

Substituting equation (7) into equation (6) and solving for K_Q,

$$K_Q = K_{Qe}\left[1 - K_{Qe}^2 \Big/ \left(\pi a F_{tu}^2\right)\right]^{-1/2} \qquad (8)$$

where

$$K_{Qe} = S_c \sqrt{\pi a \sec (\pi a/W)} \qquad (9)$$

is the usual "elastic" stress-intensity factor at failure.

In reference 8, values of fracture toughness K_Q, but not strength S_c,

were reported. However, the values of K_Q were not calculated with equa-

tions (8) and (9). Thus, values of strength were calculated with the K_Q

equations in reference 8, and then K_Q was recalculated with equations (8)

and (9).

The elastic constants and the ultimate tensile fiber strains used to cal-

culate Q_c/ε_{tuf} are given in table III. The elastic constants for the B/Al

and Gr/Pi layups were taken from references 1 and 11, respectively. For most

of the other layups, the elastic constants were not reported. They were therefore calculated with laminate analysis using the elastic constants in table III for [0] layups. The same elastic constants were used for all Gr/Ep laminates with the same proportion of 0°, ±45°, and 90° plies, even though they were not all made from the same material system nor with the same stacking sequence and number of plies. The elastic constants in table III for [0] E-Gl/Ep, B/Ep, and S-Gl/Ep were taken from references 6, 10, and 12, respectively. Those for [0] Gr/Ep were determined from tests of $[0]_{8T}$ T300/5208 specimens (63 percent fiber volume fraction) by the author.

The failing strains of unidirectional unnotched laminates were used as values of ε_{tuf} in table III. Because the failing strains were usually not reported, they were estimated from stress-strain plots or were calculated as the ratio of strength to Young's modulus. (The stress-strain curves for the unidirectional laminates were very linear to failure.)

For the S-Gl-Gr/Ep hybrid laminates, the value of ε_{tuf} for either S-Gl/Ep or Gr/Ep was used to calculate Q_c/ε_{tuf}, depending on the particular laminate. (See table III.) When all the 0° plies are S-Gl/Ep, the principal load-carrying plies are S-Gl/Ep, and the ε_{tuf} of S-Gl/Ep is used. But when the 0° plies are half S-Gl/Ep and half Gr/Ep, the 0° Gr/Ep plies are the principal load-carrying plies because the graphite plies carry 2.5 times the load that the S-glass plies carry, but fail at about one-third the strain. Thus, the ε_{tuf} of Gr/Ep was used for the laminates with half-and-half 0° plies, and likewise for the $\left[\pm45_{Gl}/\pm45_{Gr}\right]_S$ laminates.

Values of Q_c/ε_{tuf} could also be calculated this way for hybrid layups in which the S-glass fibers (or some other fibers) are uniformly integrated into the graphite plies rather than segregated into individual plies.

The values of Q_c/ε_{tuf} in table I are shown in the bar graph in figure 4. The data are grouped by material and all layups, except for those belonging to [0/±45/90], are identified. The space in figure 4 is insufficient to identify individually the numerous [0/±45/90] layups. The values of Q_c/ε_{tuf} between 1.25 and 1.75$\sqrt{mm}$ (the shaded band) represent data between the 20th and 73rd percentiles, respectively (53 percent of the data). (See the normal probability plot in figure 5.) Laminates with Q_c/ε_{tuf} values in this band failed basically by self-similar crack extension, at least in the macroscopic sense, with little crack-tip damage. The data outside this band are more scattered and are associated mostly with laminates that had variant failure modes, such as splitting. If the Q_c/ε_{tuf} values outside this band are excluded, the values within the band have a coefficient of variation of 0.10, which is about the same as that for F_{tu} values of unidirectional laminates. Therefore, the parameter Q_c/ε_{tuf} accounts very well for the effects of layup and material when the crack extension is self-similar and the crack-tip damage is relatively small.

The value of Q_c/ε_{tuf} for the 47th percentile, which is midway between the 20th and 73rd percentiles, is 1.50$\sqrt{mm}$. This value should be a good estimate of the average or representative value for all of the materials.

The large value of Q_c/ε_{tuf} for the $[\pm45]_{2S}$ B/Al layup was reported in reference 1 to have been caused by overall yielding, especially for specimens with short slits. (The stress-strain behavior of all the B/Al layups in reference 1 was nonlinear, but to a lesser degree for layups with a larger proportion of 0° plies. However, except for the $[\pm45]_{2S}$ laminates, the effect of the nonlinear stress-strain behavior was mostly eliminated by using remote failing strains rather than strengths to calculate Q_c.) The large values of Q_c/ε_{tuf}

for the $[0/\pm45/90]_{2S}$ and $[0/90]_{4S}$ Gr/Ep layups in reference 6 are anomalous. Data from other references gave much lower values.

The other values of Q_c/ε_{tuf} above the 73rd percentile in figure 4 are mostly associated with layups that split extensively, such as hybrid layups and Gr/Ep layups with a large proportion of 0° plies or 0° plies grouped together. As noted previously, splits reduce local fiber stresses. Therefore, when laminates split, the stress-intensity factor overestimates local fiber stresses, and values of K_Q and thus Q_c are greatly elevated.

For many of the B/Ep layups, the values of Q_c/ε_{tuf} in figure 4 are below the 20th percentile. For the $\left[90_2/0_2/90_2/\overline{\mp45}\right]_S$ layup, the unnotched tensile specimens, as well as the specimens with crack-like slits, failed with low strains in the 0° fibers--much lower than ε_{tuf}. In fact, the F_{tu} values reported in reference 10 for many of the fiber-dominated layups do not follow the rule of mixtures very well--not nearly as well as the various fiber-dominated Gr/Ep layups in table I. (The F_{tu} value for $[90/0]_{2S}$ in table I was taken from ref. 13 because the unnotched specimens in ref. 10 failed at a grip.) The low values of Q_c/ε_{tuf} for the $[\pm45/0/\pm45/\overline{0}]_S$ and $[90/-45/90/45]_S$ layups could be anomalous since only a couple of specimens were tested.

There is no evidence that the low values of Q_c/ε_{tuf} for the $\left[0_2/\pm45\right]$ and $[0/\pm45]_{2S}$ Gr/Ep layups are anomalous. The data come from three sources and represent many specimens, and the F_{tu} values follow the rule of mixtures fairly well. Perhaps the Q_c/ε_{tuf} values are low because the matrix damage at the slit ends is relatively small. (Compare radiographs in figure 3 for the $[45/0/-45/0]_{2S}$ Gr/Ep specimen with those in figures 1 and 2 for the $[45/0/-45/90]$ Gr/Ep specimens.)

It is interesting that, for a value of $Q_c/\varepsilon_{tuf} = 1.5\sqrt{mm}$, the character-istic distance $\bar{d}_o$ calculated with equation (A2) is quite small, only 0.36 mm. This distance is only about two to two-and-one-half times the spacing of the boron fibers or the thickness of the Gr/Ep plies. The smallest distance one would expect is one fiber spacing for boron fibers or, for tows of small fibers like graphite, one ply thickness. Therefore, when crack-tip damage is small at failure, the singular strain field given by the stress-intensity factor approxi-mates the actual strains near the slit ends fairly well.

Also, for laminates damaged by ballistic impact, values of K_Q/F_{tu} for B/Ep and Gr/Ep (ref. 14) agree quite well with those calculated using a Q_c/ε_{tuf} value of $1.5\sqrt{mm}$. Assuming that the unnotched strengths follow the rule of mixtures $\left(F_{tu} = E_y\varepsilon_{tuf}\right)$, equation (3) gives

$$K_Q/F_{tu} = \left(Q_c/\varepsilon_{tuf}\right)/\xi \tag{10}$$

Equation (10) predicts that K_Q/F_{tu} varies with layup. For the various layups in reference 14, ξ varies from 0.54 to 0.94. Therefore, equation (10) pre-dicts values of K_Q/F_{tu} from 1.6 to $2.8\sqrt{mm}$, which compare well with the values of 2.6 to $3.1\sqrt{mm}$ from reference 14, at least for the larger values. The lowest predicted values of K_Q/F_{tu} are associated with laminates that have a large proportion of 0° plies. For these laminates, as noted previously, splitting usually makes the measured values of K_Q higher than the predicted values. Notice also that the range of K_Q/F_{tu} values for different layups is drasti-cally diminished by splitting. Therefore, experiments, based on data from these laminates alone, might lead to the conclusion that K_Q/F_{tu} is independent of layup, which contradicts equation (10) and contradicts the observed results from tests of laminates that do not split.

16

It was shown in reference 1 that the crack-tip damage size ρ_c given by equation (7) agreed well with the extent of stable fiber breaks in 0° plies of $\left[0_i/\pm45_j\right]_S$ B/Al laminates. For [0/±45/90] Gr/Ep layups, equation (7) gives $\rho_c = 2.6$ mm, using properties of the material in table II from manufacturer B. This prediction falls within the 2 to 3 mm range of 0° fiber breaks shown previously in figures 1 and 2. Therefore, equation (7) predicts the extent of stable crack extension in the 0° plies of Gr/Ep, at least for [0/±45/90] layups, as well as B/Al.

STRENGTH PREDICTIONS WITH Q_c/ε_{tuf}

Method for Calculating Strength

Strengths of epoxy specimens made with the various layups in table I were predicted assuming $Q_c/\varepsilon_{tuf} = 1.5\sqrt{mm}$. Solving equations (3), (8), and (9) for strength and replacing Q_c by $1.5\varepsilon_{tuf}$,

$$S_c\sqrt{\sec\ (\pi a/W)}/F_{tu} = \left\{1 + \pi a\left[\xi F_{tu}/\left(1.5\varepsilon_{tuf}E_y\right)\right]^2\right\}^{-1/2} \tag{11}$$

The right-hand side of equation (11) is independent of specimen width, and, for laminates that follow the rule of mixtures $\left(F_{tu} = \varepsilon_{tuf}E_y\right)$, is independent of the ultimate tensile strength F_{tu}. It mainly depends on slit length and ξ, which depends mainly on laminate orientation. Thus, for convenience, the strength ratio on the left-hand side of equation (11) rather than the absolute strength was used to compare measured and predicted strengths. All measured strengths shown hereinafter are generally averages of two or three tests.

Equation (11), which is based upon failing stress, does not predict strengths for nonlinear laminates like B/Al as well as the procedure in reference 1, which is based upon failing strain. Therefore, the procedure in

reference 1 was also used here. First, the failing-strain ratio was predicted by

$$\varepsilon_c \sqrt{\sec\,(\pi a/W)}/\varepsilon_{tu} = \left\{1 + \pi a\left[\xi\varepsilon_{tu}/\left(1.5\varepsilon_{tuf}\right)\right]^2\right\}^{-1/2} \qquad (12)$$

Then, the strength ratio was predicted with the Ramberg-Osgood stress-strain equation from reference 15. Because the stress-strain relationship is nonlinear, the calculation of $S_c\sqrt{\sec\,(\pi a/W)}/F_{tu}$ from $\varepsilon_c\sqrt{\sec\,(\pi a/W)}/\varepsilon_{tu}$ will depend upon a/W. But preliminary calculations with different values of a/W indicated that the dependency on a/W was very small and could be neglected.

Comparisons of Predicted and Measured Strengths

Fiber-dominated layups.- Strength ratios are plotted against slit length in figure 6 for [0/±45/90], [0/±45], $\left[0_2/\pm4\overline{5}\right]$, and [0/90] layups made of several different materials. Predictions were essentially identical for several materials in figure 6(a). Except for the $[0/\pm45]_{2S}$ and $[0/\pm45/0]_{2S}$ Gr/Ep layups in figures 6(b) and 6(c), the predicted and measured strength ratios agree fairly well. However, for the $[0/\pm45]_{2S}$ and $[0/\pm45/0]_{2S}$ Gr/Ep layups, the predicted strength ratios were noticeably higher than the measured strength ratios. The low values of Q_c/ε_{tuf} noted before reflect these low values of strength.

The $\left[0_2/\pm4\overline{5}\right]_S$ B/Ep specimen in figure 6(c) with the longest slit (2a = 25.4 mm) split at the ends of the slit in the 0° plies. The splits extended to the ends of the specimen before the specimen failed. Thus, the stress on the net section (compare the circular symbol to the dashed curve) was close to the ultimate tensile strength. Splitting was not reported in the $\left[0_2/\pm4\overline{5}\right]_S$ B/Ep specimens with slits shorter than 25.4 mm.

18

As predicted, the strength ratios in figure 6 for a given laminate orientation do not strongly depend on the type of composite material—whether the matrix is epoxy, polyimide, or aluminum, or whether the fibers are graphite, boron, or E-glass. In fact, the differences in the curves are probably less than normal experimental scatter (10 percent coefficient of variation) combined with differences among fiber volume fractions of the various laminates (usually not reported). All of the layups are very notch sensitive. Slits longer than 15 mm reduce the strength 50 percent or more.

Matrix-dominated layups.- Predicted and measured strength ratios are plotted in figure 7 for [±45] layups made of Gr/Ep, B/Ep, and B/Al, which are matrix dominated. An unusually large width effect was reported in reference 1 for [±45]$_{2S}$ B/Al specimens, which had widths of 19.1, 50.8, and 101.6 mm. For a given slit length, strength increased with specimen width more than predicted by the theory of elasticity. (Two symbols are shown in figure 7 for specimens with 2a = 5.1 mm because they had different widths.) Despite this width effect, the measured and predicted strength ratios for [±45]$_{2S}$ B/Al agree fairly well. Also, the strength ratios are surprisingly low for [±45]$_{2S}$ B/Al, as low as those for the fiber-dominated layups in figure 6.

On the other hand, as predicted, the strength ratios for the [±45]$_{2S}$ epoxy layups are much higher than those for the [±45]$_{2S}$ B/Al. For the 25.4- and 88.9-mm-wide [±45] epoxy layups, the predicted strength ratios result in net-section stresses greater than F_{tu}. (Solid curves are above the dashed curves.) Therefore, the actual strengths for the 25.4- and 88.9-mm-wide [±45] epoxy specimens were limited by the small net-section areas and were thus lower than the predicted strengths. (Strangely enough, the net-section stresses for the 25.4-mm-wide Gr/Ep specimens were considerably greater than F_{tu}.) However, for

the 254-mm-wide Gr/Ep specimens, the net-section stresses are below F_{tu}, and the measured and predicted strength ratios agree almost exactly. Therefore, the general fracture toughness parameter correctly predicted the large difference between strength ratios for [±45] layups with epoxy and aluminum matrices. Because the fiber strains reached the predicted critical levels, fracture of these [±45] layups is actually "fiber dominated," except maybe for the small epoxy specimens.

The minimum specimen width that will result in net-section stresses smaller than F_{tu} can be predicted with equations (3) and (8). Setting $S_c = F_{tu}(1 - 2a/W)$ and solving for width,

$$W \geq \left[\left(Q_c/\varepsilon_{tuf}\right)\left(E_y\varepsilon_{tuf}/F_{tu}\right)\Big/(\xi\pi a/W)\right]^2\left[\left(1 - \frac{2a}{W}\right)^{-2}\cos\,(\pi a/W) - 1\right] \tag{13}$$

Using properties in tables I and III for [±45] Gr/Ep laminates, equation (13) gives minimum widths between 84 and 153 mm for values of $2a/W$ between 0 and 0.5. And for [0/±45/90] Gr/Ep laminates, equation (13) gives minimum widths between 10 and 19 mm. Therefore, much wider specimens are required for [±45] Gr/Ep than for [0/±45/90] Gr/Ep.

Hybrid layups.- The predicted and measured strength ratios are plotted in figure 8 for the hybrid laminates in reference 7. Except for the $\left[0_{G1}/\pm45_{Gr}/90_{Gr}\right]_S$ hybrid specimens, the measured strength ratios are considerably larger than the predicted ratios, as reflected in the large Q_c/ε_{tuf} values in table I. As discussed previously, the large strengths were caused by extensive splitting at the slit ends in the 0° plies, like that shown in figure 3. However, for the $\left[0_{G1}/\pm45_{Gr}/90_{Gr}\right]_S$ hybrid specimens, the predicted

20

and measured strength ratios agree very well. Thus, in this laminate, damage

at the slit ends must have been relatively small up to failure. Unlike the

all-graphite $[\pm45]_{2S}$ specimens in reference 7, the $\left[\pm45_{G1}/\pm45_{Gr}\right]_S$ hybrid

specimens delaminated extensively at the slit ends well before overall failure.

Consequently, the net-section stress in the $\left[\pm45_{G1}/\pm45_{Gr}\right]_S$ hybrid specimens

was close to F_{tu} in figure 8.

Even though the strengths of most of the hybrid specimens were not pre-

dicted well, the trends were. The strengths of hybrid layups and all-Gr/Ep

layups in the table below are in the correct proportions. Notice that, as

predicted, there was little or no actual improvement in strength of the

$\left[0_{G1}/\pm45_{Gr}/0_{Gr}/90_{Gr}\right]_S$ and $\left[\pm45_{G1}/\pm45_{Gr}\right]_S$ hybrid layups over the corresponding

all-Gr/Ep layups.

Hybrid Layup	$\left(S_c\right)_{\text{Hybrid}} \Big/ \left(S_c\right)_{\text{All-Gr/Ep}}$	
	Predicted	Experimental
$\left[0_{2G1}/\pm45_{Gr}\right]_S$	1.67	2.29
$\left[0_{G1}/\pm45_{Gr}/90_{Gr}\right]_S$	1.94	1.73
$\left[0_{G1}/\pm45_{Gr}/0_{Gr}/90_{Gr}\right]_S$	.80	.89
$\left[\pm45_{G1}/\pm45_{Gr}\right]_S$	.74	1.19

Effect of layup.- The predicted and measured strength ratios are replotted

in figure 9 for the various Gr/Ep layups. Only one curve is shown for the

$[0/\pm45/90]$ layups and the $[0/\pm45/0]_{2S}$ layup because the predictions are virtu-

ally the same. Except for the $[0/\pm45/0]_{2S}$ and $[0/\pm45]_{2S}$ layups, the order of

the curves is correct. For the $[0/\pm45/0]_{2S}$ and $[0/\pm45]_{2S}$ layups, the measured

strengths are lower than the predicted strengths, as noted previously. (The

measured and predicted strengths might be in better agreement if actual elastic

constants had been available for predicting the strengths.)

As predicted, the overall effect of layup in figure 9 is large. The

effect among the fiber-dominated layups is much smaller, but is still signifi-

cant (greater than the effect of material in figure 6). The strength ratios of

$[0/90]_{4S}$ specimens are about two-thirds those of $[0/\pm45/90]$ specimens. For

long slits, they are predicted to be about one-half. As shown in the appendix,

the "point stress" criterion cannot predict the effect of layup in figure 9

because it is based on laminate stresses at the slit ends, which do not depend

upon layup.

CONCLUDING REMARKS

Values of Q_c/ε_{tuf}, where Q_c is the general fracture toughness parameter

and ε_{tuf} is the ultimate tensile strain of the fibers, were calculated from

test data for various $\left[0_i/\pm45_j/90_k\right]$ symmetric and balanced laminates made with

different fiber and matrix materials. The materials were graphite/epoxy (Gr/Ep),

boron/epoxy (B/Ep), E-glass/epoxy (E-Gl/Ep), S-glass-graphite/epoxy (S-Gl-Gr/Ep),

graphite/polyimide (Gr/Pi), and boron/aluminum (B/Al). In all, there were 44

combinations of materials and layups. The tests were conducted on specimens of

various sizes containing central crack-like slits of various lengths.

Within ordinary scatter, the data indicate that Q_c/ε_{tuf} is a constant for

all laminates that do not split extensively at the crack tips or have other

deviate failure modes. A representative value of Q_c/ε_{tuf} is $1.5\sqrt{mm}$. Values

of Q_c/ε_{tuf} are significantly above $1.5\sqrt{mm}$ for laminates that split extensively

22

at the ends of the crack-like slit. Laminates that usually split are made of epoxy with a large proportion of 0° plies, with 0° plies grouped together, or with 0° plies of S-glass/epoxy (hybrid). The value of Q_c/ε_{tuf} for $[\pm45]_{2S}$ B/Al specimens with short slits is also elevated due to overall yielding.

Radiography and crack-opening displacement (COD) measurements are good nondestructive test methods for monitoring crack-tip damage during fracture tests. Moreover, for $[0/\pm45/90]$ Gr/Ep specimens, the COD measurements reveal the actual extent of broken 0° fibers at the crack tip.

Strengths were predicted for specimens made with the various materials and layups and compared to the measured strengths. A single value of $Q_c/\varepsilon_{tuf} = 1.5\sqrt{mm}$ was used for all the materials and layups. Except for laminates that split extensively, the measured and predicted strengths agree fairly well, even for $[\pm45]$ layups. When laminates split, predictions are conservative.

Except for the $[\pm45]$ and hybrid layups, ratios of cracked to uncracked strengths are not significantly affected by the type of material. For the $[\pm45]$ layups, the ratios of cracked to uncracked strengths for epoxy specimens are much larger than those for B/Al specimens. (For net-section stresses at failure to be lower than the uncracked strength, the width of $[\pm45]$ epoxy specimens has to be nearly 10 times that of $[\pm45]$ B/Al specimens or fiber-dominated specimens.) For some of the hybrid layups, the cracked strengths are about twice those of the same all-Gr/Ep layups. For the others, they are about the same or less. The general fracture toughness parameter correctly predicts these trends. However, the predicted strengths of the hybrid layups are usually conservative due to extensive splitting.

Layup (laminate orientation) has a significant effect on the ratio of cracked to uncracked strength. For a 25 mm slit, the ratio for a $[0/90]$ Gr/Ep

specimen is nearly one-fourth that for a [±45] Gr/Ep specimen and nearly one-half that for a [0/±45/90] Gr/Ep specimen. The differences increase with slit length. The general fracture toughness parameter predicts these layup effects. The "point stress" and "average stress" criteria predict no layup effect.

APPENDIX

COMPARISON OF "POINT STRESS" CRITERION AND GENERAL FRACTURE

TOUGHNESS PARAMETER

It is important to note the differences between the general fracture toughness parameter Q_c and the "point stress" criterion of Whitney and Nuismer. The "point stress" criterion, as originally presented in reference 2, assumes that the distance d_o to the point where the laminate stress is equal to F_{tu} is "a material property independent of laminate geometry and stress distribution." Data in reference 2 indicate that values of d_o for $[0/\pm45]$ E-Gl/Ep specimens with holes and $[0/\pm45]$ Gr/Ep specimens with crack-like slits are equal. Since then, other investigations (refs. 6, 8, and 16) have reported experimental data that indicate d_o (or a_o for the "average stress" criterion) may be equal for different materials as well as for different layups, at least for fiber-dominated layups.

One can infer a constant characteristic distance from the general fracture toughness parameter Q_c as well. Considering only the singular component, the principal fiber strains directly ahead of the crack tip are given by

$$\varepsilon_1 = Q_c/\sqrt{2\pi x} \tag{A1}$$

where x is the distance from the crack tip. If $\bar{d}_o$ is the distance to the point where $\varepsilon_1 = \varepsilon_{tuf}$, it follows from equation (A1) that

$$\sqrt{2\pi\bar{d}_o} = Q_c/\varepsilon_{tuf} \tag{A2}$$

Therefore, if Q_c/ε_{tuf} is a constant for all layups and materials, then the characteristic distance $\bar{d}_o$ is a constant as well.

APPENDIX

Although the "point stress" criterion and the general fracture toughness

parameter both assume or imply a constant characteristic distance, the criteria

are quite different. First, unlike the "point stress" criterion, the general

fracture toughness parameter is not limited to fiber-dominated layups. Second,

the general fracture toughness parameter predicts a much more significant layup

effect, even for fiber-dominated layups.

The layup effect can be seen as follows. Considering only the singular com-

ponent of stress, the "point stress" criterion gives d_o in terms of K_Q as

$$\sqrt{2\pi d_o} = K_Q/F_{tu} \tag{A3}$$

(The effect of including only the singular component is negligible when

$a \gg d_o$.) Whereas, substituting equation (1) into equation (A2), the general

fracture toughness parameter gives

$$\sqrt{2\pi \bar{d}_o} = \left[K_Q/F_{tu}\right]\left[\xi F_{tu}/\left(E_y \varepsilon_{tuf}\right)\right] \tag{A4}$$

A comparison of equations (A3) and (A4) shows that the "point stress" criterion

predicts that K_Q/F_{tu} is independent of layup and material, whereas the general

fracture toughness parameter predicts that K_Q/F_{tu} varies inversely with

$\xi F_{tu}/\left(E_y \varepsilon_{tuf}\right)$. Similarly, the "point stress" criterion predicts that the ratio

of cracked to uncracked strength S_c/F_{tu} is independent of layup and material,

whereas the general fracture toughness parameter predicts that S_c/F_{tu} varies

approximately inversely with $\xi F_{tu}/\left(E_y \varepsilon_{tuf}\right)$.

The factor ξ depends mainly on layup (laminate orientation). It appears

in the results for the general fracture toughness parameter, and not the "point

stress" criterion, because the principal fiber strains depend on layup, whereas

the laminate stresses do not. For fiber-dominated layups, the values of ξ in table III range between 0.48 and 0.95 and, for [±45], are as low as 0.22.

The factor $F_{tu}/\left(E_y \varepsilon_{tuf}\right)$ should theoretically be unity for fiber-dominated layups that are linear to failure. For most of the fiber-dominated layups in table I, it ranges between 0.85 and 1.00. (Most of the values below 0.85 are associated with the nonlinear B/Al and hybrid layups and with the B/Ep layups. As noted before, the B/Ep results seem anomalous.) Since the values of $\xi F_{tu}/\left(E_y \varepsilon_{tuf}\right)$ range approximately between one-half and unity for the fiber-dominated layups in table III, the strengths calculated with the general fracture toughness parameter will be as much as two times those calculated with the "point stress" criterion. Similarly, the characteristic distances calculated with the two criteria differ by as much as a factor of 4. For the [±45] epoxy layups, the differences can be much larger.

Also, note that the general fracture toughness parameter can be applied to laminates containing holes and other types of notches just like the "point stress" criterion.

REFERENCES

1. Poe, C. C., Jr.; and Sova, J. A.: Fracture Toughness of Boron/Aluminum Laminates with Various Proportions of 0° and ±45° Plies. NASA TP-1707, 1980.

2. Whitney, J. M.; and Nuismer, R. J.: Stress Fracture Criteria for Laminated Composites Containing Stress Concentrations. J. Compos. Mater., vol. 8, July 1974, pp. 253-265.

3. Zweben, Carl: An Approximate Method of Analysis for Notched Unidirectional Composites. Eng. Fract. Mech., vol. 6, no. 1, Mar. 1974, pp. 1-10.

4. Goree, James G.; and Gross, Robert S.: Analysis of a Unidirectional Composite Containing Broken Fibers and Matrix Damage. Eng. Fract. Mech., vol. 13, no. 2, June 1980, pp. 563-578.

5. Morris, D. H.; and Hahn, H. T.: Fracture Resistance Characterization of Graphite/Epoxy Composites. Composite Materials: Testing and Design (Fourth Conference), Spec. Tech. Publ. 617, American Soc. Testing & Mater., 1977, pp. 5-17.

6. Nuismer, R. J.; and Whitney, J. M.: Uniaxial Failure of Composite Laminates Containing Stress Concentrations. Fracture Mechanics of Composites, Spec. Tech. Publ. 593, American Soc. Testing & Mater., 1975, pp. 117-142.

7. Walter, R. W.; and June, R. R.: Designing for Improved Fracture Strength in Advanced Composites. Proceedings of the 23rd National SAMPE Symposium and Exhibition, Selective Application of Materials for Products and Energy, vol. 23, 1978, pp. 877-892.

8. Yeow, Y. T.; Morris, D. H.; and Brinson, H. I.: A Correlative Study Between Analysis and Experiment on the Fracture Behavior of Graphite/Epoxy Composites. J. Testing and Eval., vol. 7, no. 2, Mar. 1979, pp. 117-125.

9. Daniel, Isaac M.: Strain and Failure Analysis of Graphite/Epoxy Plates with Cracks. Exp. Mech., July 1978, pp. 246-252.

10. Durchlaub, Erwin C.; and Freeman, Richard B.: Design Data for Composite Structure Safelife Prediction. AFML-TR-73-225 (vol. II), Air Force Materials Laboratory, 1974.

11. Awerbuch, Jonathan: Deformation Characteristics and Failure Modes of Notched Graphite Polyimide Composites at Room and Elevated Temperatures. NASA CR-159375, 1981.

12. Goree, James G.: Preliminary Investigation of Crack Arrest in Composite Laminates Containing Buffer Strips. NASA CR-3000, 1978.

13. Advanced Composites Design Guide. Volume IV - Materials. Third Edition
    (Third Revision). Contract No. F33615-74-C-5075, Air Force Flight Dyna-
    mics Laboratory, Sept. 1976, p. 4.1.1-2.

14. Avery, J. G.; and Porter, T. R.: Comparisons of the Ballistic Impact
    Response of Metals and Composites for Military Aircraft Applications.
    Foreign Object Impact Damage to Composites, Spec. Tech. Publ. 568,
    American Soc. Testing & Mater., 1975, pp. 3-29.

15. Sova, J. A.; and Poe, C. C., Jr.: Tensile Stress-Strain Behavior of Boron/
    Aluminum Laminates. NASA TP-1117, 1978.

16. Caprino, G.; Halpin, J. C.; and Nicolais, L.: Fracture Mechanics in Com-
    posite Materials. Composites, vol. 10, no. 4, Oct. 1979, pp. 223-227.

TABLE I.- ULTIMATE TENSILE STRENGTHS AND GENERAL FRACTURE

TOUGHNESS VALUES FOR VARIOUS MATERIALS AND LAYUPS

Laminate orientation	F_{tu}, MPa	Q_c, $\sqrt{mm}$	Q_c/ε_{tuf}, $\sqrt{mm}$
T300/5208 Graphite/Epoxy (ref. 5)			
$[0/\pm45]_{2S}$	541	0.01091	1.091
$[0/90/\pm45]_S$	454	.01752	1.752
T300/5208 Graphite/Epoxy (ref. 6)			
$[0/\pm45/90]_{2S}$	494	0.02483	2.483
$[0/90]_{4S}$	637	.02521	2.251
T300/5208 Graphite/Epoxy (ref. 7)			
$[\pm45]_{2S}$	172	0.01566	1.566
$[45/0/-45/90]_S$	375	.01586	1.586
$[90/\pm45/0]_S$	343	.01768	1.768
$[\pm45/0/90]_S$	365	.01443	1.443
$[\pm45/90/0]_S$	452	.01375	1.375
$[0/\pm45/90]_S$	462	.01600	1.600
$[0_2/\pm45/90]_S$	585	.02199	2.199
$[0_2/\pm45/0_2/90]_S$	702	.02035	2.035
$[0_4/\pm45/90]_S$	742	.03877	3.877

TABLE I.- Continued

Laminate orientation	F_{tu}, MPa	Q_c, $\sqrt{mm}$	Q_c/ϵ_{tuf}, $\sqrt{mm}$
T300/934 Graphite/Epoxy (ref. 8)			
$[0]_{16T}$	1427	0.03002	3.002
$[0/\pm45/0]_{2S}$	724	.01021	1.021
$[0/90]_{4S}$	793	.01645	1.645
$[\pm45]_{4S}$	167	.01110	1.110
T300/SP-286 Graphite/Epoxy (ref. 9)			
$[0/\pm45/90]_S$	502	0.01904	1.904
T300-S-Glass/5208 Graphite-S-Glass/Epoxy (ref. 7)			
$[0_{2Gl}/\pm45_{Gr}]_S$	787	0.07053	2.519
$[0_{Gl}/\pm45_{Gr}/90_{Gr}]_S$	367	.04496	1.606
$[0_{Gl}/\pm45_{Gr}/0_{Gr}/90_{Gr}]_S$	368	.02561	2.561
$[\pm45_{Gl}/\pm45_{Gr}]_S$	168	.02798	2.798
Celion 6000/PMR-15 Graphite/Polyimide (ref. 11)			
$[0/45/90/-45]_{2S}$	433	0.01756	1.756
T300/5208 Graphite/Epoxy (Manufacturer D)			
$[45/0/-45/0]_{2S}$	750	0.01000	1.000
$[45/0/-45/90]_{2S}$	504	.01607	1.607
T300/5208 Graphite/Epoxy (Manufacturer B)			
$[45/0/-45/90]_{2S}$	458	0.01773	1.773

31

TABLE I.- Concluded

Laminate orientation	F_{tu}, MPa	Q_c, $\sqrt{mm}$	Q_c/ε_{tuf}, $\sqrt{mm}$
E-Glass/5208 E-Glass/Epoxy (ref. 6)			
$[0/\pm45/90]_{2S}$	320	0.02946	1.473
$[0/90]_{4S}$	423	.03256	1.628
Avco Boron (4 mil)/Epoxy (ref. 10)			
$[0/\pm45/90]_S$	439	0.01089	1.452
$[0_2/\pm45]_S$	827	.01032	1.376
$[0/45/0/-45]_S$	789	.009778	1.304
$[\pm45/0_2]_S$	808	.01078	1.437
$[\pm45/0/\pm45/\overline{0}]_S$	491	.007190	.959
$[90/0]_{2S}$	[a]655	.008819	1.176
$[0/90/0_2/(\pm45)_2]_S$	567	.009710	1.295
$[0_2/90_2/0_2/\pm45]_S$	553	.01127	1.503
$[90_2/0_2/90_2/\mp45]_S$	169	.005107	.681
$[90/-45/90/45]_S$	123	.005161	.688
$[\pm45]_{2S}$	141	.00925	1.233
B5.6/6061-F Boron/Aluminum (ref. 1)			
$[0]_{6T}$	1672	0.01328	1.679
$[0_2/\pm45]_S$	800	.01068	1.351
$[\pm45/0_2]_S$	911	.01074	1.358
$[0/\pm45]_S$	581	.01250	1.581
$[\pm45]_{2S}$	221	.02156	2.726

[a]Reference 13.

TABLE II.- T300/5208 GRAPHITE/EPOXY TEST DATA

W, mm	2a, mm	S_c, MPa	K_Q, MPa$\sqrt{\text{mm}}$
[45/0/-45/0]$_{2S}$ (Manufacturer D)			
25.4	7.6	284	1130
25.4	7.6	274	1090
50.8	15.2	239	1320
50.8	15.2	333	1950
			[a]1370
[45/0/-45/90]$_{2S}$ (Manufacturer D)			
22.2	7.6	254	1130
50.8	15.2	237	1230
50.8	15.2	230	1190
101.6	30.5	157	1220
			[a]1190
[45/0/-45/90]$_{2S}$ (Manufacturer B)			
50.8	8.5	245	1090
50.8	16.9	206	1300
50.8	16.9	207	1310
101.6	33.8	165	1400
101.6	33.8	172	1470
			[a]1310

[a]Average.

33

TABLE III.- ULTIMATE TENSILE FIBER-STRAIN AND ELASTIC CONSTANTS FOR VARIOUS

MATERIALS AND LAYUPS

Material	Laminate orientation	ε_{tuf}	E_y, GPa	E_x, GPa	ν_{yx}	G_{xy}, GPa	ξ
Gr/Ep	[0]	0.010	129.4	10.86	0.3118	5.70	0.9097
	[0/±45/90]		51.40	51.40	.3065	19.67	.6935
	[0/90]		70.54	70.54	.0483	5.70	.9517
	[0/±45]$_{2S}$		56.87	25.40	.6857	24.33	.5418
	[0$_2$/±45]		75.35	23.36	.6476	19.67	.6394
	[0$_2$/±45/90]$_S$		67.00	44.60	.3068	16.88	.7497
	[0$_4$/±45/90]		84.83	35.64	.3072	13.68	.8009
Gr/Ep	[±45]	0.010	19.75	19.75	.7336	33.65	.2664
E-Gl/Ep	[0]	0.020	38.60	8.27	0.2600	4.140	----
	[0/±45/90]$_{2S}$		18.96	18.96	.2695	7.469	0.7305
E-Gl/Ep	[0/90]$_{4S}$	0.020	23.58	23.58	.9175	4.140	.9082

TABLE III.- Continued

Material	Laminate orientation	ε_{tuf}	E_y, GPa	E_x, GPa	ν_{yx}	G_{xy}, GPa	ξ
B/Ep	[0]	0.0075	206.9	20.70	0.2700	7.310	0.9146
	[0/±45/90]$_S$		81.66	81.66	.3210	30.91	.6790
	$\left[0_2/\pm45\right]$		118.6	37.95	.6620	30.91	.6255
	[±45/0/±45/$\overline{0}$]$_S$		76.73	39.66	.7299	41.63	.4752
	[90/0]$_{2S}$		114.4	114.4	.4911	7.310	.9509
	$\left[0/90/0_2/(\pm45)_2\right]_S$		101.8	60.13	.4324	30.91	.6678
	$\left[0_2/90_2/0_2/\pm45\right]_S$		122.5	76.99	.2195	19.11	.8259
	$\left[90_2/0_2/90_2/\overline{\mp45}\right]_S$		76.99	122.5	.1380	19.11	.8259
	[90/-45/90/45]$_S$		37.95	118.6	.2119	30.91	.4897
B/Ep	[±45]$_{2S}$	0.0075	26.07	26.07	.7832	54.50	.2168
S-Gl-Gr/Ep	$\left[0_{Gl}\right]$	0.028	51.02	11.03	0.2900	4.48	---
	$\left[0_{2Gl}/\pm45_{Gr}\right]_S$	.028	36.26	20.67	.6413	19.06	0.5159
	$\left[0_{Gl}/\pm45_{Gr}/90_{Gr}\right]_S$	.028	31.91	48.69	.3054	19.37	.6221
	$\left[0_{Gl}/\pm45_{Gr}/0_{Gr}/90_{Gr}\right]_S$	.010	51.33	43.83	.3057	16.63	.7175
S-Gl-Gr/Ep	$\left[\pm45_{Gl}/\pm45_{Gr}\right]_S$	.010	17.15	17.15	.6853	23.91	.3147

TABLE III.- Concluded

Material	Laminate orientation	ε_{tuf}	E_y, GPa	E_x, GPa	ν_{yx}	G_{xy}, GPa	ξ
B/Al	$[0]_{6T}$	0.007908	237.3	143.1	0.2049	48.68	0.8409
	$[0_2/\pm 45]_S$		176.2	130.1	.2513	65.82	.7841
	$[\pm 45/0_2]_S$		177.5	134.7	.2519	65.82	.7806
	$[0/\pm 45]_S$		159.2	129.5	.2911	71.43	.7375
B/Al	$[\pm 45]_{2S}$	0.007908	126.9	126.2	.3247	82.94	.6771
Gr/Pi	$[0/45/90/-45]_{2S}$	0.010	45.85	----	0.339	----	0.661

RADIOGRAPH   PHOTOGRAPH AFTER PLY REMOVAL
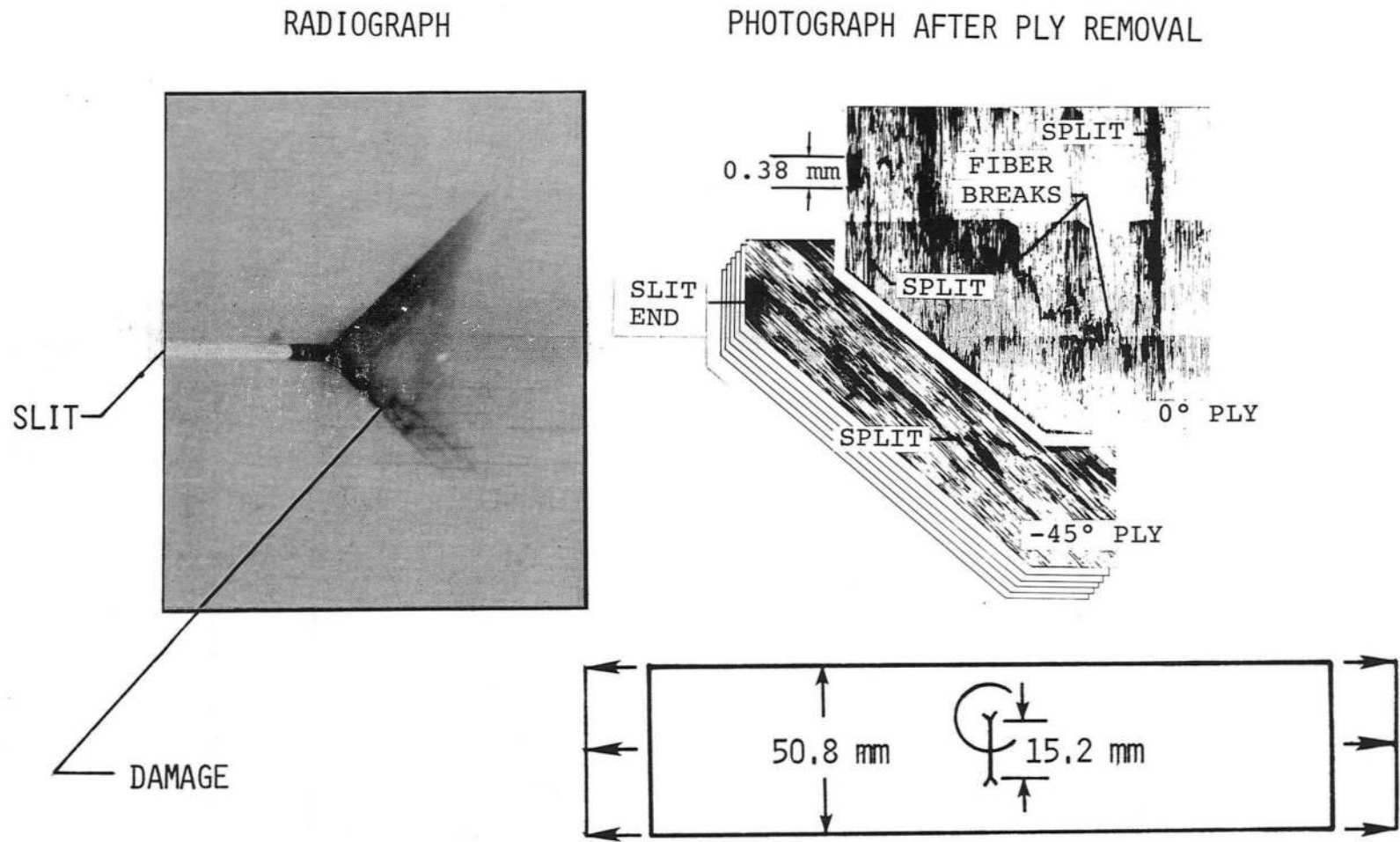
Figure 1.- Crack-tip damage in a [45/0/-45/90]$_S$ Gr/Ep specimen loaded to
95 percent of estimated failing load.
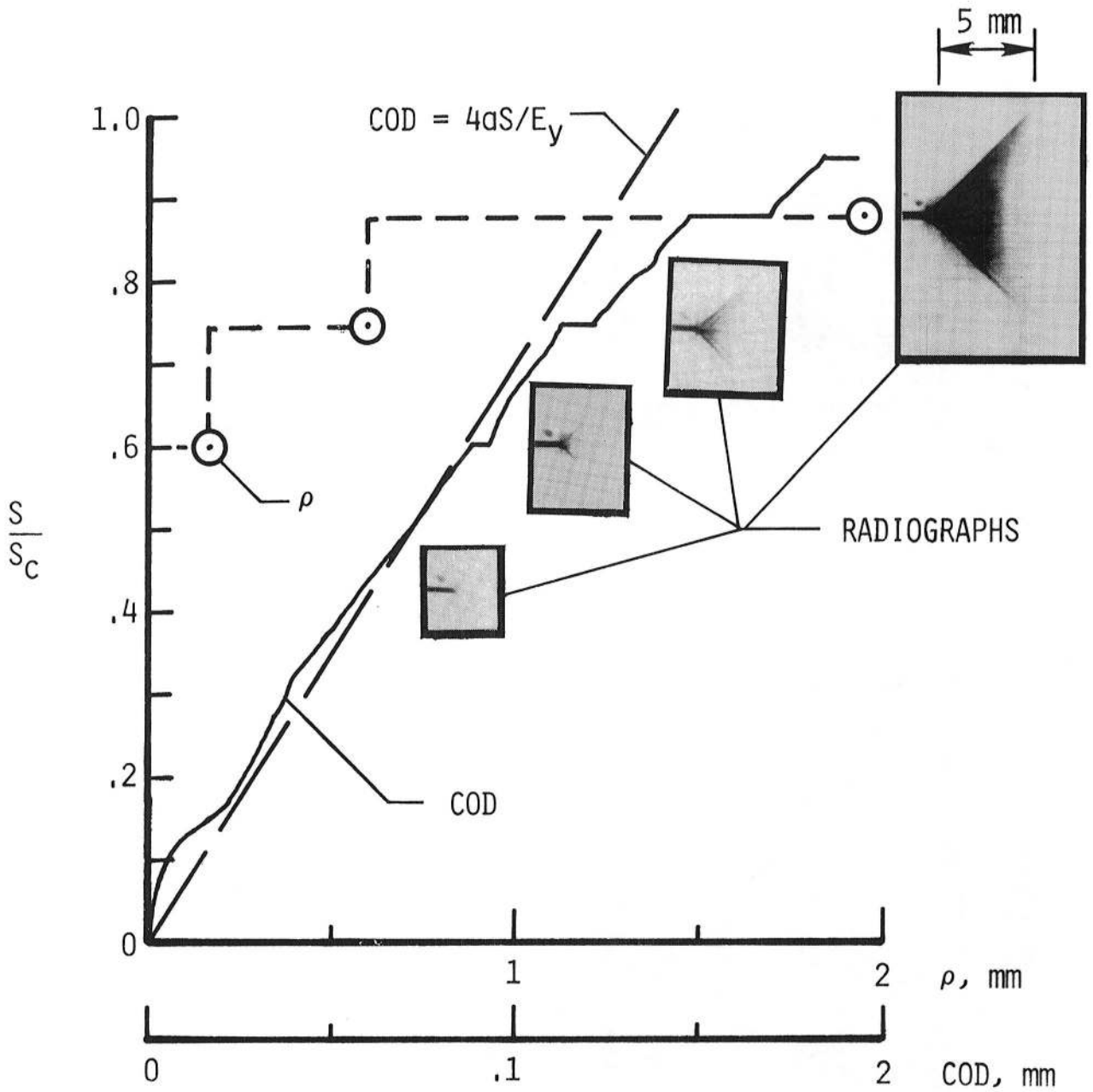
Figure 2.- Crack-tip damage ρ and COD curve of a
$[45/0/-45/90]_{2S}$ Gr/Ep specimen.

$2a = 16.9$ mm, $W = 50.8$ mm, and $S_c = 208$ MPa.

$[45/0/-45/0]_{2S}$
ALL-GR/EP

STRESS = 196 MPa $(0.820 \ S_c)$
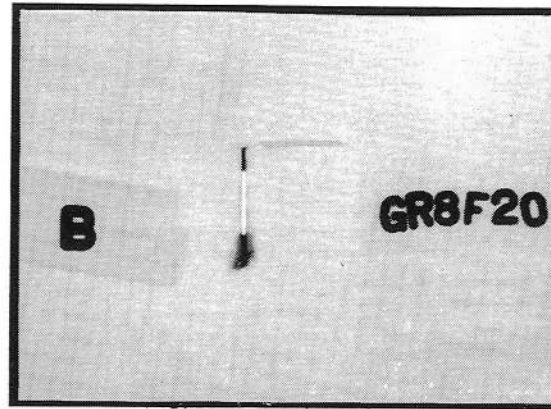
$\left[45_{GR}/0_{GL}/-45_{GR}/0_{GL}\right]_{2S}$

S-GL-GR/EP
HYBRID
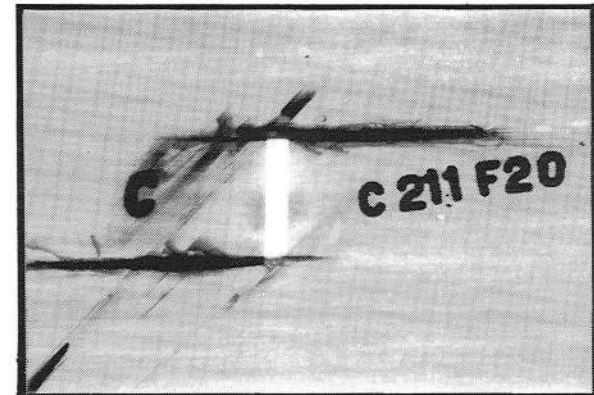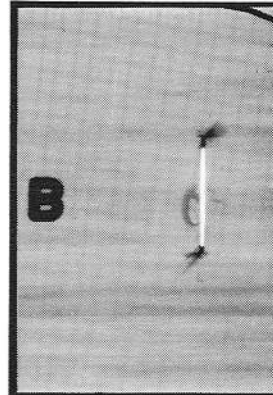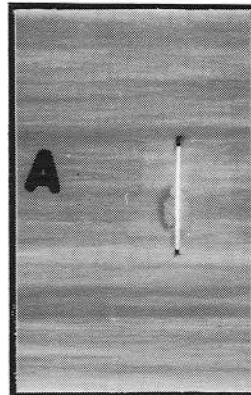
STRESS =
IN MPa

196 $(0.397 \ S_c)$ 294 $(0.595 \ S_c)$ 392 $(0.794 \ S_c)$

Figure 3.- Crack-tip damage in a hybrid and an all-graphite/epoxy specimen.
$2a = 15.2$ mm,   W = 50.8 mm.
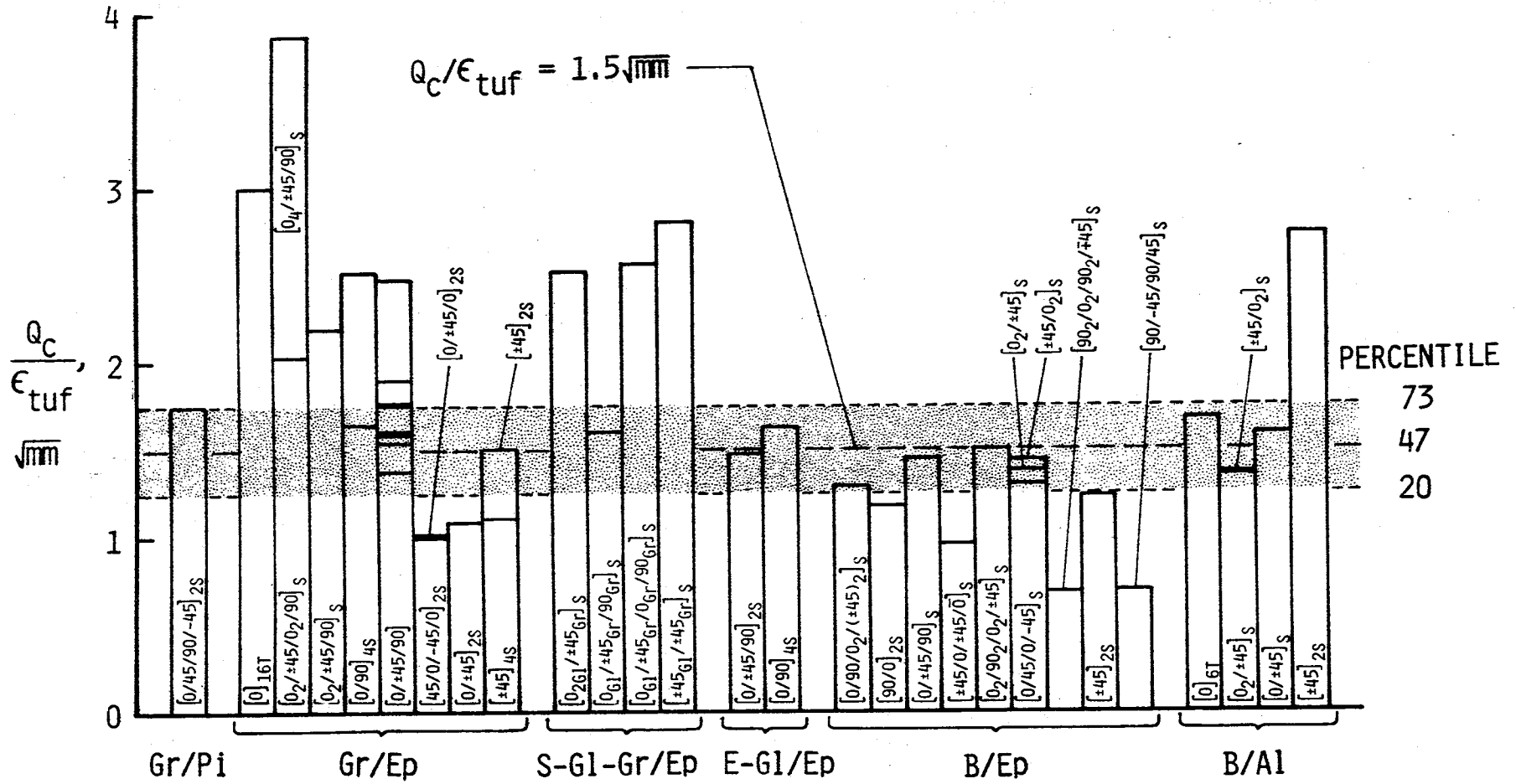
Figure 4.- Values of Q_c/ϵ_{tuf} for various composite materials and layups.
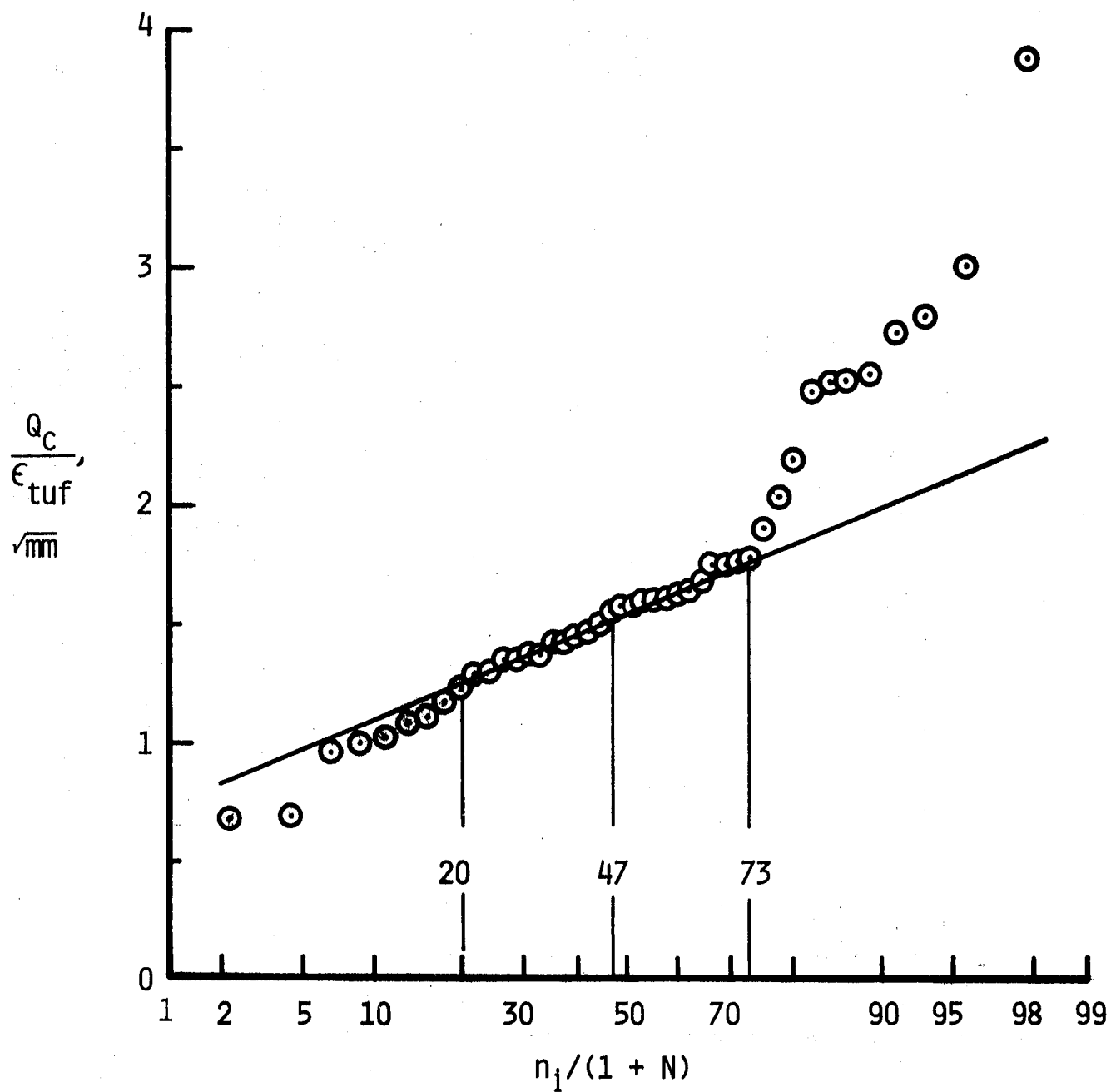
Figure 5.- Normal probability plot of Q_c/ϵ_{tuf} values.
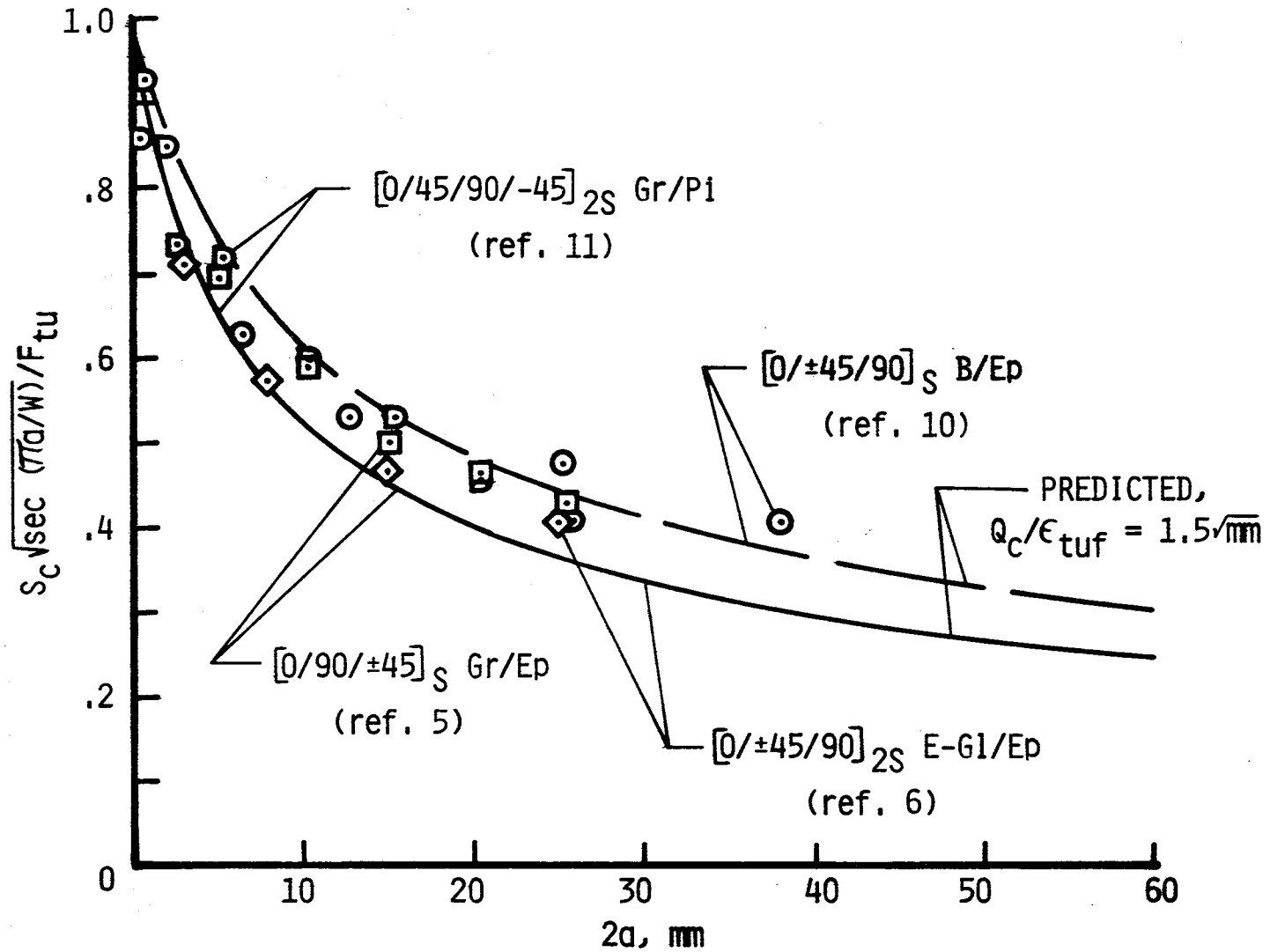
(a) [0/±45/90] layups.

Figure 6.- Predicted and measured strengths of specimens with different materials.
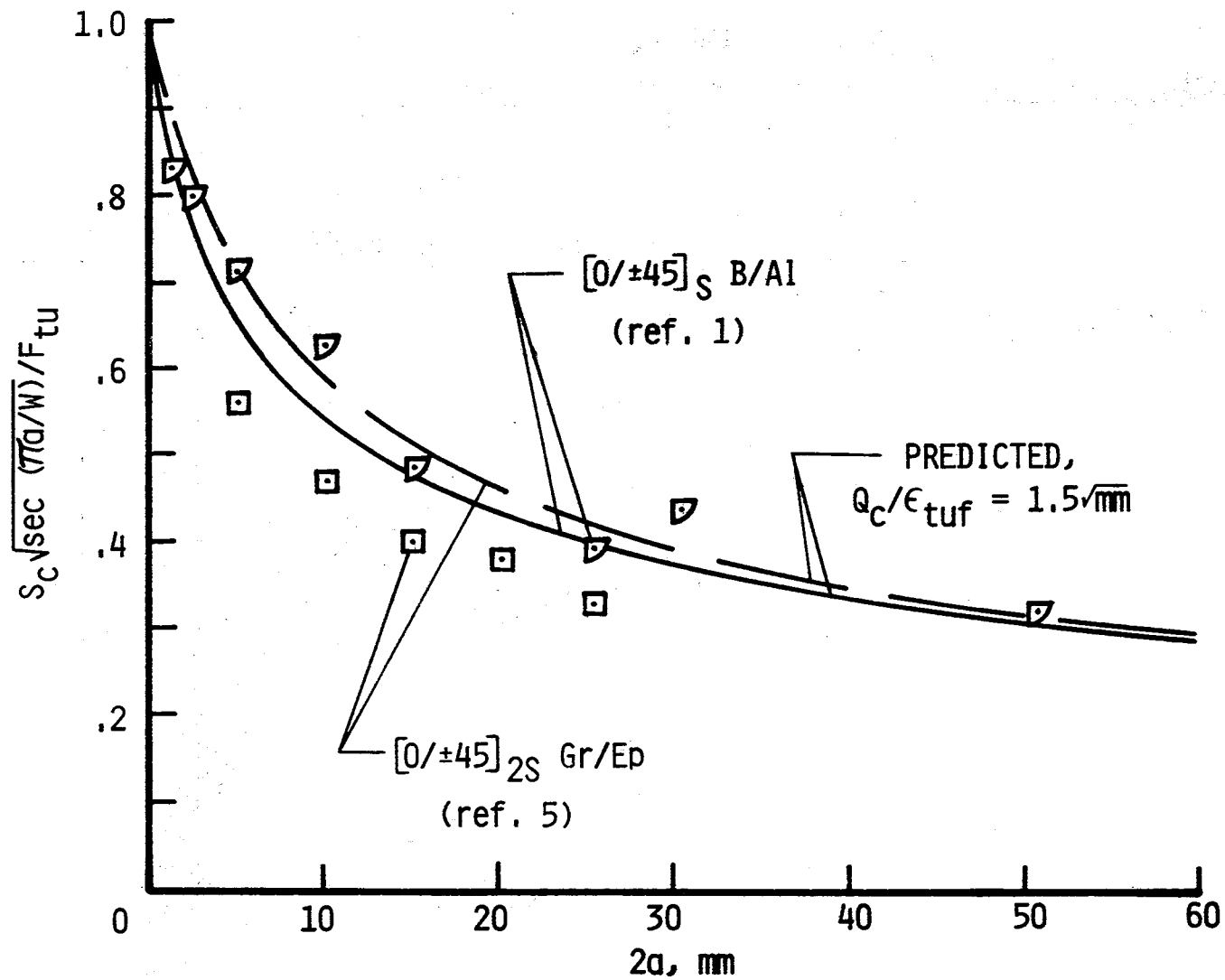
(b) [0/±45] layups.

Figure 6.- Continued.
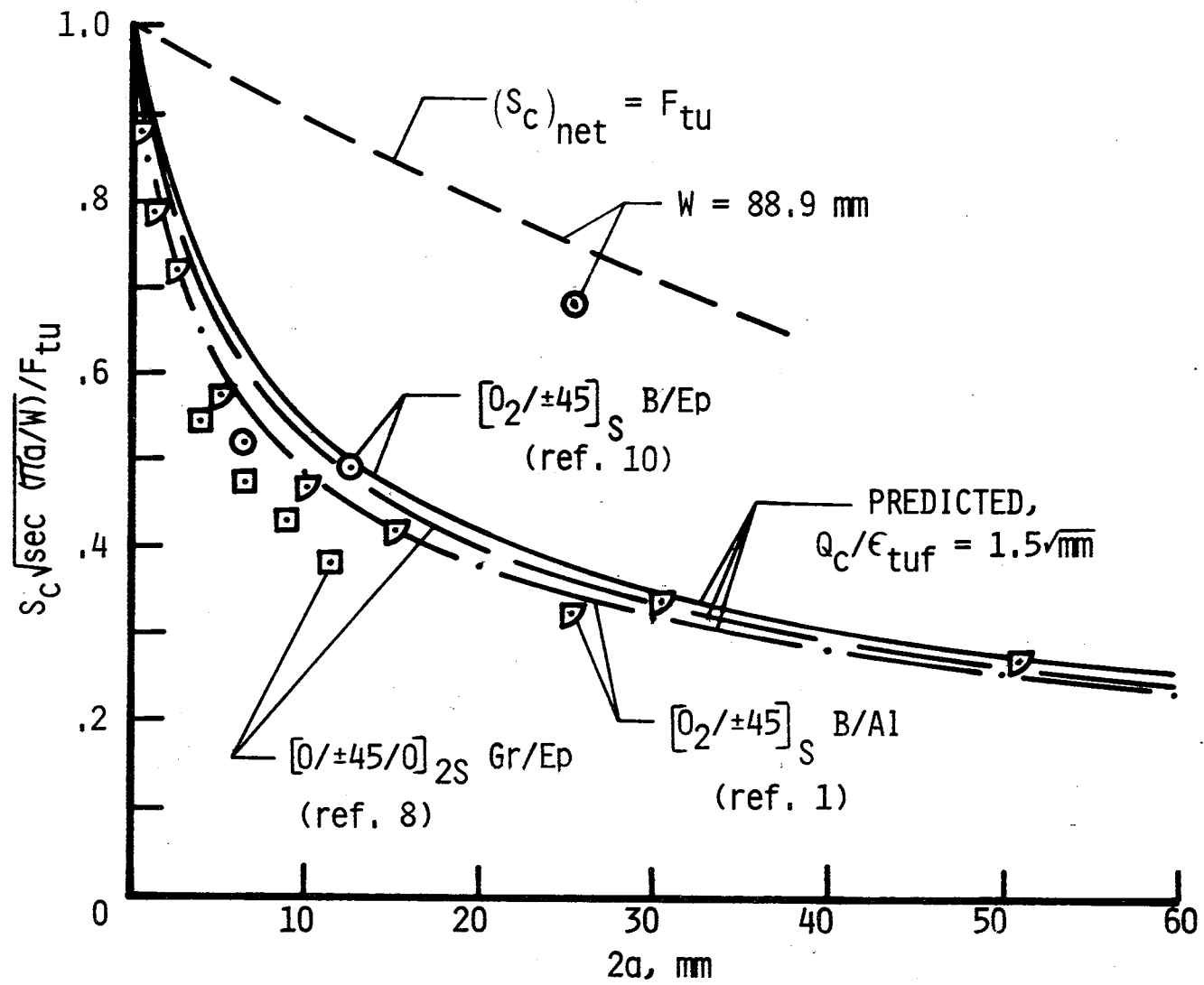
(c) $[0_2/\pm45]$ layups.

Figure 6.- Continued.
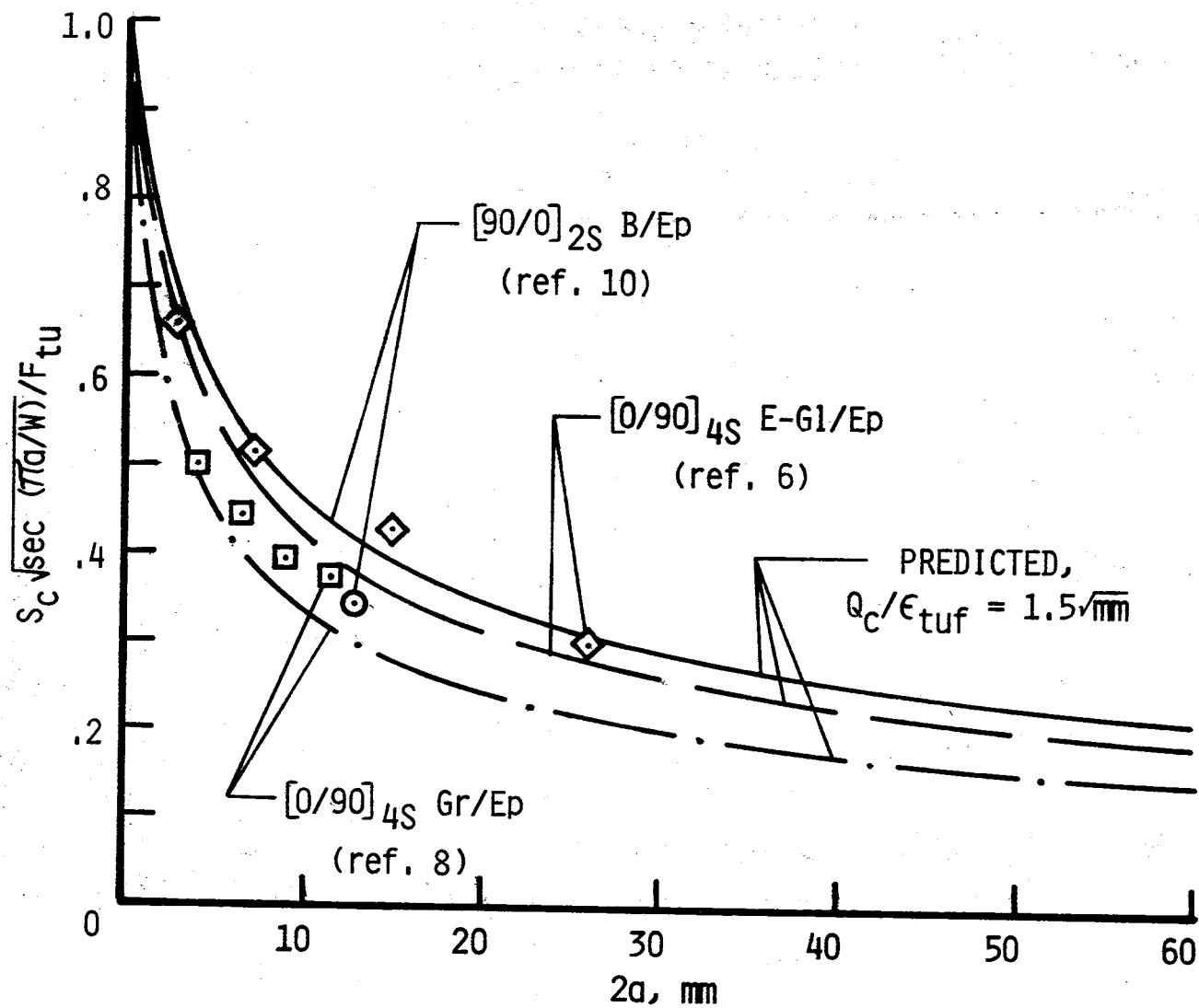
(d) [0/90] layups.

Figure 6.- Concluded.
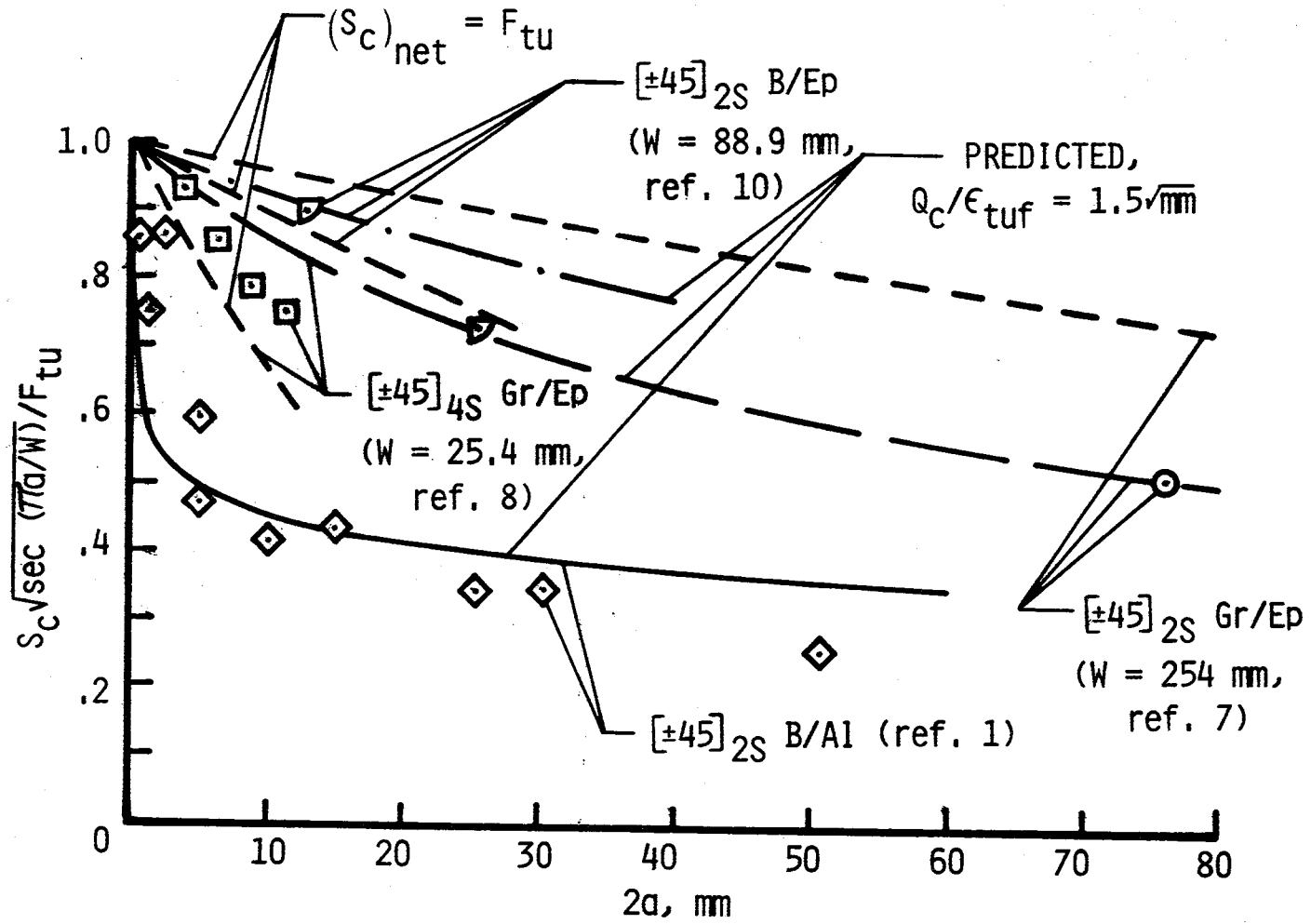
Figure 7.- Predicted and measured strengths of $[\pm 45]$ specimens with different materials.
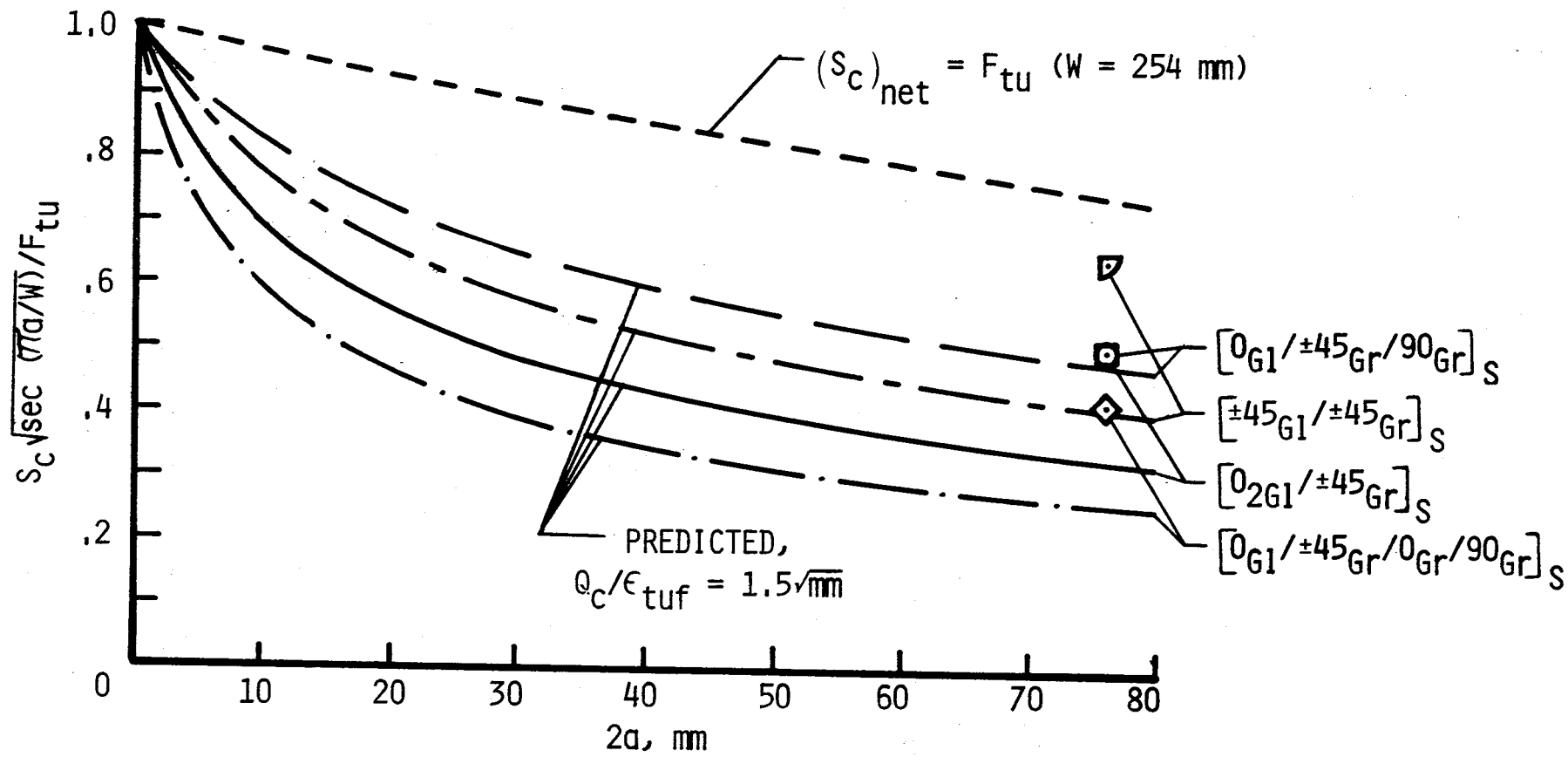
Figure 8.- Predicted and measured strengths of hybrid specimens with different layups (ref. 7).
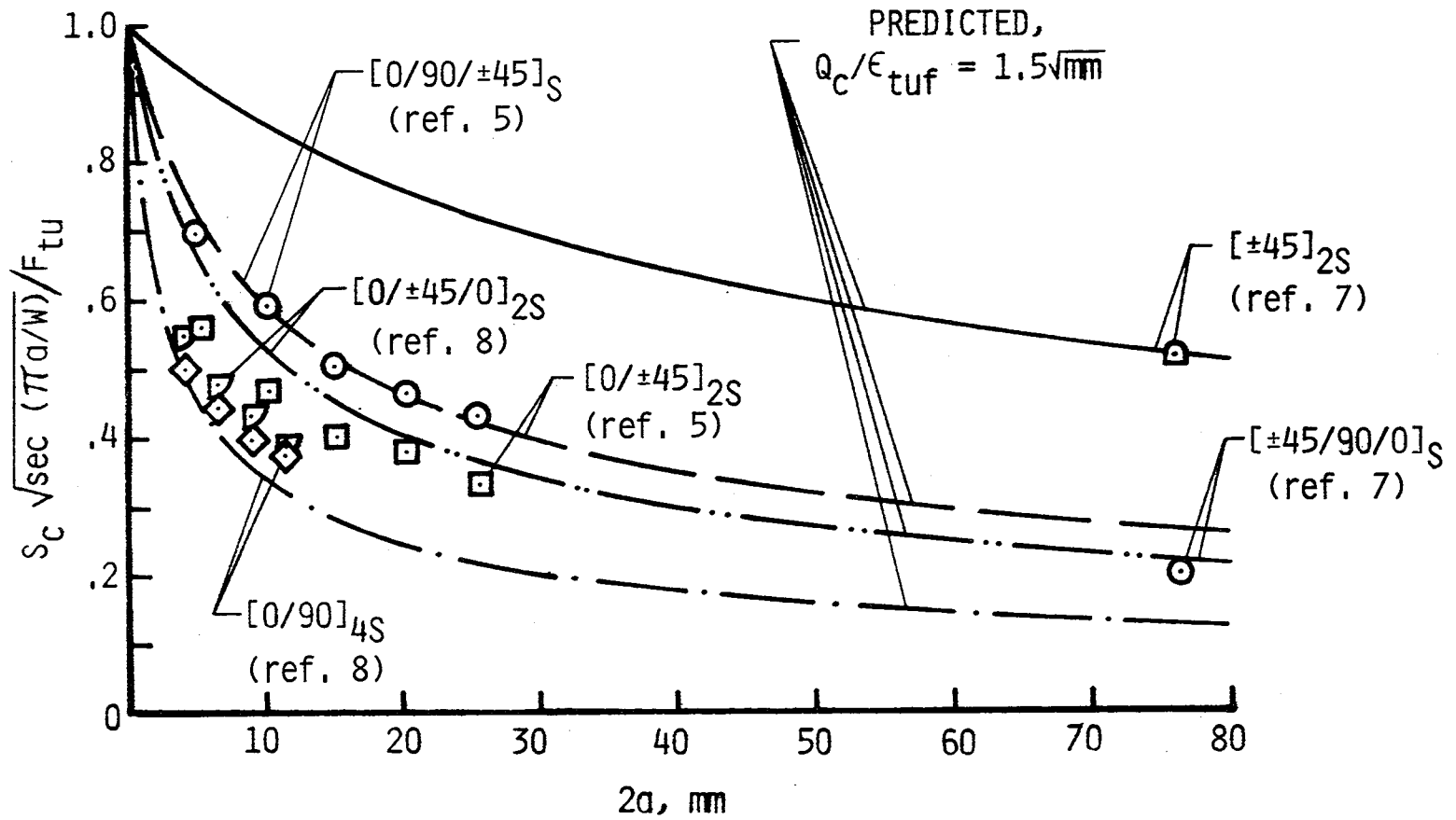
Figure 9.- Predicted and measured strengths of Gr/Ep specimens with different layups.

1. Report No. NASA TM-81911	2. Government Accession No.	3. Recipient's Catalog No.
4. Title and Subtitle A SINGLE FRACTURE TOUGHNESS PARAMETER FOR FIBROUS COMPOSITE LAMINATES		5. Report Date March 1981
		6. Performing Organization Code 505-33-33-05
7. Author(s) C. C. Poe, Jr.		8. Performing Organization Report No.
9. Performing Organization Name and Address NASA Langley Research Center Hampton, VA 23665		10. Work Unit No.
		11. Contract or Grant No.
12. Sponsoring Agency Name and Address National Aeronautics and Space Administration Washington, DC 20546		13. Type of Report and Period Covered Technical Memorandum
		14. Sponsoring Agency Code

16. Abstract

A general fracture toughness parameter Q_c was previously derived and verified to be a material constant, independent of layup, for centrally cracked boron/aluminum composite specimens. The specimens were made with various proportions of $0°$ and $±45°$ plies. Moreover, a limited amount of data indicated that the ratio Q_c/ε_{tuf}, where ε_{tuf} is the ultimate tensile strain of the fibers, might be a constant for all composite laminates, regardless of material and layup. In that case, a single value of Q_c/ε_{tuf} could be used to predict the fracture toughness of all fibrous composite laminates from only the elastic constants and ε_{tuf}.

To verify that Q_c/ε_{tuf} is indeed a constant, values of Q_c/ε_{tuf} were calculated for centrally cracked specimens made from graphite/polyimide, graphite/epoxy, E-glass/epoxy, boron/epoxy, and S-glass-graphite/epoxy materials with numerous $[0_i/\pm45_j/90_k]$ layups. Within ordinary scatter, the data indicate that Q_c/ε_{tuf} is a constant for all laminates that did not split extensively at the crack tips or have other deviate failure modes.

Using a single value of Q_c/ε_{tuf} for all the layups and materials, strengths were predicted for the test specimens. The predicted and test values agree well except for laminates that split extensively. Then, the predicted strengths are usually conservative.

17. Key Words (Suggested by Author(s)) Composite materials Strength Crack-like flaws Predictions Centrally cracked specimens Fracture toughness		18. Distribution Statement Unclassified - Unlimited Subject Category 39

19. Security Classif. (of this report) Unclassified	20. Security Classif. (of this page) Unclassified	21. No. of Pages 48	22. Price* A03